MARINTEK

Norwegian Marine Technology Research Institute

Postal address:
P.O.Box 4125 Valentinlyst
NO-7450 Trondheim, NORWAY

Location:
Marine Technology Centre
Otto Nielsens veg 10

Phone: +47 7359 5500
Fax: +47 7359 5776

http://www.marintek.sintef.no

Enterprise No.: NO 937 357 370 MVA

SINTEF

MARINTEK REPORT

TITLE

Expert evaluation of Boussole buoy design

AUTHOR(S)

Øyvind Hellan, Bernt Leira, Rolf Baarholm, Svein Erling Heggelund, Halvor Lie

CLIENT(S)

ESA

FILE CODE	CLASSIFICATION	CLIENTS REF.	
700203	Internal	Pascal Lecomte	
CLASS. THIS PAGE	ISBN	PROJECT NO.	NO. OF PAGES/APPENDICES
Internal		700203	24 / 9
REFERENCE NO.		PROJECT MANAGER (NAME, SIGN.)	VERIFIED BY (NAME, SIGN.)
P		Øyvind Hellan	Halvor Lie
REPORT NO.	DATE	APPROVED BY (NAME, POSITION, SIGN.)	
700203.00:01	2002-12-01	Oddvar I. Eide, Division Director	

ABSTRACT

The present report describes the findings of an expert evaluation of the overall design of the Boussole buoy.

The results of the initial deployment indicate that the buoy design is successful with respect to the functional requirements, and that the present design has the required stability for the radiographic measurements.

The present investigations indicate the tube/sphere intersection as the most probable cause of failure. Analyses indicate that the stresses in the aluminium skin can be in a range that will cause fatigue failure after relatively few months at sea.

The Kevlar cable is identified as a second weak link in the design, from transportation, installation and recovery perspective. Kevlar is a brittle material, and fails easily under compression or bending. The Kevlar cable has already failed twice, the second time causing loss of the complete system (during recovery).

The following areas that should be evaluated in the development of the new design:

- The present design for the top mast (carbon fibre and instrumentations) seems well suited for the purpose, and need not be changed. A less costly material than carbon fibre can however be considered without compromising buoy stability, provided the lower part of the buoy is modified to maintain the hydrostatic stiffness, e.g. by increasing the distance from fairlead to the centre of the buoy.
- The buoyancy body could with benefit be made in synthetic foam (e.g. polyurethane) with a protective skin. Several commercial buoyancy products are available, which could easily be adapted to the present purpose.
- The lower part of the mast (aluminium part) should be re-designed to fit the new buoyancy body or bodies.
- Polyester rope should be considered for the mooring line instead of Kevlar.

KEYWORDS	ENGLISH	NORWEGIAN
GROUP 1	Marine Technology	Marin teknikk
GROUP 2	Buoy	Bøye
SELECTED BY AUTHOR	Mooring	Forankring
	Structural assessment	Konstruktiv vurdering

CONTENTS

1. SUMMARY

The present report describes the findings of an expert evaluation of the overall design of the Boussole buoy.

The results of the initial deployment indicate that the buoy design is successful with respect to the functional requirements, and that the present design has the required stability for the radiographic measurements.

However, sinking of the buoy during the second deployment, and loss of the complete system during recovery operations indicate that the buoy design has serious shortcomings from an engineering perspective. Also, the documentation of the design, and the analyses/evaluations behind, are limited.

To substantiate any claims with respect to current or revised designs, MARINTEK has created a number of numerical models and performed the following analyses:

- "Global" hydrodynamic analyses of the buoy including mooring. These analyses are done to assess the hydrodynamic loading on the buoy, the response of the buoy in different sea states, and the forces generated between the different components in the system, mooring line, aluminium structure etc.
- Local analysis of the lower aluminium trusswork. These analyses are done to evaluate the capacity of the lower truss, and to determine the order of magnitude of forces transferred between the mast and the sphere
- Detail analyses of the truss/sphere intersection, to assess local plate stresses and the possibility of fatigue.

This series of analyses contain various simplifications and assumptions, and the results should be used with caution. Nevertheless, the analyses give valuable information about the main load-carrying mechanisms, and provide the order of magnitude of the forces and stresses transferred through the system.

The analyses indicate the tube/sphere intersection as a probable cause of failure. Based on the information available, the analyses suggest that the stresses in the aluminium skin can be in a range that would lead to fatigue failure after relatively few months at sea.

Our review indicate the Kevlar cable as the second weakest link in the design, not from a strength point of view, but from a transportation, installation and recovery perspective. Kevlar is a brittle material, and fails easily under compression or bending. Failure of the Kevlar cable caused loss of the complete system during last season's recovery operations.

The present work has identified the following areas that should be evaluated in the development of the new design:

- The present design for the top mast (carbon fibre and instrumentations) seems well suited for the purpose, and need not be changed. A less costly material than carbon fibre can however be considered without compromising buoy stability, provided the lower part of the buoy is modified to maintain the hydrostatic stiffness, e.g. by increasing the distance from fairlead to the centre of the buoy.
- The aluminium sphere could with benefit be replaced by a buoyancy body (or bodies) made in synthetic foam (e.g. polyurethane) with a skin in fibre-reinforced epoxy, rotationally moulded polyethylene or cast/sprayed polyurethane elastomer.
  Several commercial buoyancy products are available, which could easily be adapted to the present purpose.
- The lower part of the mast (aluminium part) should be re-designed to fit the new buoyancy body (or bodies).
- Assessment of fatigue failure should be included as part of the documentation for the future design.
- Polyester rope should be considered for the mooring line instead of Kevlar.

Our review has only identified one structural detail that can seriously affect the buoy lifetime: the transition of the aluminium tubes through the skin of the buoy. If such details are omitted in the future design, we see no reason why the structure should not confirm to the standards typically expected from marine and offshore structures.

A periodic diving inspection programme of the buoy structure is recommended for the first one or two years of deployment, e.g. coinciding with regular maintenance of the optical instruments. If inspections are successful (i.e. no findings), the intervals can be relaxed to yearly of bi-yearly intervals.

2. INTRODUCTION

ESA has asked MARINTEK to perform an expert review of the overall design of the Boussole buoy design. The study covers the following points:

- evaluation of the risks attached to the present design
- identification of the weak points in the system
- advice for making the buoy more robust
- information for estimating and maximizing the buoy lifetime

Findings and conclusion are based on the expertise and experience of senior personnel at MARINTEK and NTNU (the Norwegian University of Science and Technology) within the field of bottom-moored and fixed offshore structures.

3. BACKGROUND

In the framework of the Envisat products validation and calibration activities, ESA are involved in a project called Boussole led by the Laboratoire d'Oceanographie de Villefranche (LOV). The purpose of this project is to obtain ground truth data, through deployment of a buoy designed to measure the Ocean Colour with high accuracy. LOV has developed a new type of platform to minimise shadowing effects, to minimise perturbation of the sub-marine light field, and to provide the necessary stability of the instruments.

The buoy is a bottom-moored structure, stabilised by the buoyancy of a sphere (Ø 1.8 m) at -18 metres water depth, which supports a very slender trusswork structure penetrating the sea surface. The geometry is shown in Figure 1.

A prototype buoy was installed between Nice and Corsica, at 2400 meters water depth. The buoy was initially deployed for a three-month period in 2000 (July 20 to October 20). The buoy was again deployed on May 16 2002, but was lost between June 3 and June 15, 2002. Design premises, experiences from the initial deployment, and the events prior to loss of the buoy are summarised in Appendix A.

ESA is considering re-starting the project, but has ordered a complete review of the risks associated with the buoy design.

4. REVIEW OF CURRENT BUOY DESIGN

4.1 General

The buoy is designed to measure the Ocean Colour with high accuracy. The aim of the design is to provide a stable measurements platform for radiometric measurements, with minimal shadowing effects and minimum perturbation of the sub-marine light field.

The results of the initial deployment indicate that the buoy design is successful with respect to the functional requirements, and that the present design has the required stability for the radiographic measurements.

However, sinking of the buoy during the second deployment, and loss of the complete system during salvage operations indicate that the buoy design has some shortcomings from an engineering perspective.

4.2 Design documentation

The design documentation that has been provided to MARINTEK is limited, compared to what is usually expected for marine structures and offshore structures.

Hydrodynamic analyses

Hand calculations have been performed for the hydrodynamic properties of the buoy. That is, rigid body motions, the wave excitation, wave frequency motions, as well as mean tilt and offsets of the buoy exposed to wind and current. The following comments should be attached to these calculations:

- The calculations are done with a sphere of diameter 1.6 m instead of 1.8 m. This will significantly affect the results.
- The calculations are done with a much too high value for the axial stiffness of the Kevlar rope. This also has significant impact on the end results. An elastic modulus of 120 GPa is used for the Kevlar cable, whereas Aramid (each separate fibre) has an elastic modulus of 75-85 GPa. Also according to an e-mail received from Marc Le Boulluec, the ARALINE Kevlar rope exhibits an elongation of 0.78% for a tension of 29.4kN (3 tons). With a diameter of 13.1mm, this gives an averaged elastic modulus of 28 GPa.
- The mass of the mooring line, and the added mass (hydrodynamic mass) of the mooring line (Kevlar rope and chain) has not been included in the eigen period calculations. Thus, the eigen periods for surge and heave motions will be too short. When applying a more correct axial stiffness, the heave eigen period is located in a region where large wave excitation forces are expected. However, due to significant hydrodynamic damping, only limited dynamic amplification of motions are found.
- Wind loading has not been considered in the calculations, and the calculations for current loading disregard the current force acting on the mooring line. Computations presented below show that this might contribute considerably to the total current force.

Wave basin tests
The hydrodynamic properties have also been assessed through wave basin tests. This has not been evaluated in detail in the present study.

Structural properties
Structural calculations have been made for the top part of the buoy mast, when the buoy was re-designed in carbon composite. These were quasi-static analyses under idealised loading conditions, but indicated more than sufficient capacity.

Structural calculations were also made for the sphere, but these analyses were limited to the sphere itself without taking the tube/skin intersection into account. This detail should have been subjected to separate investigation.

4.3 Items not covered

From the documentation sent to MARINTEK, the following design effects seem to have been overlooked:

1. Some important properties of the material applied
2. Fatigue, typically caused by local stress concentrations in areas with abrupt changes in geometry.
3. Structural detailing

Item 1 relates to the fact that both Kevlar and aluminium has some special characteristics that should be considered before the material is used in engineering purposes.

Items 2 and 3 are important for the expected lifetime of the structure, especially for welded aluminium structures, which are known to be sensitive to fatigue.

4.4 Materials

The choice of material for the buoy is unconventional. Both Kevlar rope, carbon fibre and top some extent aluminium are materials that are characterised by low weight and high stiffness compared to more conventional materials used in marine and offshore structures. These materials are generally selected when one want stiff and light structures, which is not necessarily the case with the present buoy. Kevlar ropes are characterized by high axial stiffness and a high price. Moreover, Kevlar is very sensitive to compression and bending. It breaks easily. A Kevlar cable that has experienced compression has significantly reduced strength under subsequent tension loading.

This makes the handling of the cable under installation and recovery critical, and makes the system more vulnerable than necessary:

- The mooring line of the initial deployment was lost, possibly because the temporary buoyancy installed was not sufficient to ensure that the Kevlar cable was kept under tension in all situations.
- The entire buoy was lost during recovery operations because the Kevlar cable broke.

4.5 Fatigue / structural detailing

The transition of the aluminium tubes through the skin of the buoy is also a critical point in the present design. Problems are caused by un-even flow of stresses from one structural part into the other, where abrupt changes in geometry cause significant concentration of stresses in very local areas. Additional problems are caused by the welding, which inevitably introduce minute flaws within the material, and which serves as initiation points for local crack growth. Also, it may be difficult for the workshop to get perfect geometric fit between skin and tube – such misalignments are typically fixed by additional weld beads.

5. RISKS ASSOCIATED WITH CURRENT DESIGN

5.1 General

A summary of risks associated with various types of sources is given below. The probabilities of the various events are not quantified since this would require a substantial amount of data for the area under consideration.

5.2 Risk due to external sources

The following external sources of risk may be relevant:

- Impact caused by collision from drifting objects or boats. This may also include forces from fishing gear or temporary stops by small vessels.
- Extreme current and waves (extreme environmental loading which are much larger than expected). This may occur as a result of lacking environmental data or the occurrence of extreme events that are beyond statistical predictions.
- Damage by malicious intent. This is considered to be very unlikely.
- Marine microorganisms, fish and sea animals. In varying degree, marine structures do attract marine microorganisms (e.g. marine growth), fish and sea animals. The potential damage from these depends strongly on the type of materials that are used. In the Gulf of Mexico, and offshore Brazil, sharkbite is also considered a risk to fibre-rope mooring lines.

5.3 Risk due to handling

Handling of the various components e.g. during storage, transport, installation and recovery may result in local damage of the components. This may lead to immediate failure, or the result can be a local damage (including wear), which will imply reduced strength and resistance for the system during operation.

Kevlar cables are very sensitive to local damage, which may result in a significant reduction in the breaking strength of the cross-section.

5.4 Risk related to structural failure of the system components

The present system represents a “weakest link”-structural system in the sense that failure of a single component is likely to imply failure of the whole system. By components, we here understand the following: (i) Tower structure (ii) Buoy (or buoyant structural members) (iii) Mooring line (cable/chain) (iv) Anchor plate. In addition, there are interfaces between the components such as cable heads. In the following, aspects related to the risk of structural failure for each of the components and interfaces are listed:

5.4.1 Tower structure

Excessive dynamic response implying fatigue of the members or the connections. This seems to be a very unlikely cause of failure unless a very high level of dynamic amplification for the tower

is present. Failure of the tower is local in the sense that the integrity of the remaining parts of the system will be maintained. However, the sensors will be lost if the part of the tower where they are located is detached from the rest of the structure.

5.4.2 Buoy

The transition between the tower structure and the buoy is likely to be subjected to high stress concentrations. In addition, the welds may lead to a reduction of strength, somewhat depending on the procedures for welding and weld inspection. The degree of stress concentration depends strongly on the layout of the structural members inside the hull of the buoy. Failure at the surface of the buoy (e.g. caused by fatigue crack growth) will lead to leakage and water filling. This will easily lead to loss of the whole system, since the buoyancy represents the main source of stabilizing force.

5.4.3 Cable/chain

Failure of the cable/chain will lead to failure and loss of the whole system. Such a failure can be caused by local damage caused by handling e.g. during transportation or installation. Habitation by sea organisms (e.g. mussels) is also a possibility. If such organisms migrate in between fibres of a cable, shells or calcareous deposits may inflict local damages on the fibres. Furthermore, high total tension levels (sum of static plus dynamic) caused by dynamic amplification that is much higher than anticipated is also a possible cause.

It is also noted that if different metals are in contact (e.g. in the chain/wire and the component connecting the chain/wire) corrosion will easily take place. This applies e.g. to steel and titanium alloys. Since these metals are in direct contact, corrosion of the steel will easily take place unless some kind of electrically isolating material is applied. Such corrosion may lead to failure of the mooring system.

5.4.4 Anchor plate

Failure of the anchor plate can be caused by lower soil strength than assumed and/or higher tension in the chain e.g. due to significant dynamic amplification.

6. HYDRODYNAMIC ANALYSES OF CURRENT DESIGN

6.1 General

The current design as described in the received documentation has been modelled and analysed using the computer program RIFLEX. RIFLEX is a tailormade computer program for static and dynamic analysis of flexible riser systems and other slender marine structures developed by MARINTEK and the Norwegian University of Science and Technology. The program uses a specially developed finite element (FE) formulation applicable for cable-type structures with small bending stiffness and large deformations. The structures can be modelled by beam or cable elements. Environmental loading due to waves and current can be included, and the excitation forces are computed by a Morison approach. A more thorough description of RIFLEX is given in Appendix B.

The modelling of the mooring line and the buoy is described in Appendix C. RIFLEX was used to study the overall global behaviour of the buoy and bending moments at chosen positions along the buoy.

6.2 Eigenvalue analysis

Eigenvalue analysis has been performed to determine the eigen frequencies of the rigid body motion. Eigen frequencies of structural vibrations in the buoy are assumed to be much larger than the frequencies of the environmental loading, and they are thus not considered in this work.

In the following computations, E=28GPa is assumed for the Kevlar rope. This follows from the discussion in section 4.2. The natural periods for the translatory modes surge and heave have been computed by hand, while a pitch period is more difficult to predict due to strong coupling to the surge motion. The total mass involved comprises the structural mass including top end chains, the hydrodynamic mass and a fraction of mass of the kevel rope. Added mass of chain is not included. This yields:

Surge:	Tn = 121s
Heave:	Tn = 8.76s

Natural periods computed by RIFLEX are:

Surge/ pitch (eigenmode 1):	Tn = 128.4s
Pitch /surge (eigenmode 2):	Tn = 16.78s
Pitch /surge (eigenmode 3):	Tn = 8.72s
Heave (eigenmode 4):	Tn = 9.01s
Pitch/surge (eigenmode 5):	Tn = 7.26s

The natural periods calculated by hand and by RIFLEX compare well.

The analyses show a coupling between surge and pitch, and eigen modes contain contributions from both degrees of freedom. The shapes of the eigenmodes are shown in Figure 12-Figure 16. The heave motion (eigenmode 4) is uncoupled from surge and pitch. The pitch period is more difficult to predict due to strong coupling to the surge motion. Above three different natural periods are indicated for the pitch motion.

The eigen periods calculated here differ significantly from the ones determined by Genimar. Especially, the heave eigenperiod is critical. For the present calculations, the heave period is located in a frequency domain where large wave excitation forces are expected. If the buoy has low damping in heave, large heave motions / dynamic loads in the buoy structure and in the mooring line might occur due to ressonance. This could be critical for both the strength of the system and for fatigue.

6.3 Simulations of buoy behaviour in irregular sea

Simulations of the global behaviour of the buoy in irregular seas have been performed. Data for the zero-upcrossing period and the significant wave period for approximately three years of measurements in the region of the buoy have been studied. From this three representative sea states have been chosen. These are:

Sea state no. 1: T_Z= 7.0s and H_s=1.5m
Sea state no. 2: T_Z= 9.0s and H_s=3.5m
Sea state no. 3: T_Z=10.0s and H_s=6.0m

The former represents a typical operational sea state in which the buoy motions must be small enough for the instruments to give satisfactory results. Sea state no. 2 represents a typical large sea state that occurs rather often, while the latter represents an extreme winter storm sea state. The buoy and the mooring system should be designed to withstand the wave loading from this latter sea state. The magnitude of sea state no. 3 is based on a rough extrapolation from the most severe sea states in the measurements, which are approximately characterized by T_Z=10s and H_s=5m. Consequently, the return period associated with sea state no. 3 is not known.

A Pierson-Moscowitz model spectrum is used to describe the waves.

Three hours simulations are performed and the motion of the buoy, the tension in the top and bottom of the Kevlar rope as well as the bending moments in selected cross-sections of the buoy are studied. The global coordinate system used in the model has the *xy*-plane in the mean free surface and the *z*-axis pointing upwards. A positive heave displacement is thus upward and a positive pitch means top of buoy bows toward positive *x*-axis. The waves propagate along the positive *x*-axis.

Tables containing main statistical results are presented in Appendix D. Figure 17 and Figure 18 show how the standard deviation of the heave and pitch motions vary with the significant wave height.

After the initial deployment the design of the buoy was modified. The lower aluminium truss beams were lengthened by 1m, and the upper beams shortened correspondingly. Consequently, 1m increase in the distance from the fairlead to the centre of the buoy. This was done to increase the roll/pitch stiffness of the buoy. Computations of the behaviour of the new buoy configuration in sea state no. 2 have been performed. These are denoted Case 4 in the results in Appendix D. One can note in Figure 17 and Figure 18 that the altered design does not affect the heave response much, but the pitch response is significantly reduced.

The spectrum of heave motions for seastate no 1 is shown in Figure 25. There is no pronounced peak around the heave eigen period. This indicates thath the damping of the system is relatively high, and that the system will not experience any critical dynamic amplification in heave.

Plots of selected times series are presented in Appendix F-Appendix I.

6.4 Calculations of buoy exposed to current

In the Genimar report “Note Technique G1298/BSMEM-02” assessment of horizontal- and vertical displacement and mean tilt of the buoy due to constant current is described. The computation of the drag force on the buoy in that report is reasonable, but the drag force on the chains and the Kevlar rope is disregarded. This will not affect the results for the mean tilt angle, but the drag on the mooring line might be very important for the horizontal offset and thus the vertical setdown of the buoy.

Computations of the buoy exposed to current only are performed using RIFLEX in a static analysis. As in the Genimar studies, current velocities of 0-0.5m/s are studied. Different current profiles are investigated. In the computations presented in Figure 19-Figure 21, a constant current extending from the free surface all the way to sea floor is used. The results reported by Genimar are included in the plots. The present computations using RIFLEX gives a much larger horizontal offset due to the mean current loading. Consequently, the setdown of the buoy is much larger in the present study. It should be noted that Genimar only accounts for the setdown due to the mean tilt angle of the buoy and not the contribution from the offset. The latter contribution will by far be the dominant one. The mean tilt angle is little affected by the drag force on the mooring line, and thus the results from the RIFLEX analysis and the Genimar results compare very well for the tilt angle.

This also indicates that both the mass distribution and the drag coefficients used in the present model coincide with the Genimar model.

The current close to the free surface give the most important contributions to the horizontal off set and thus the vertical set down of the buoy. However, to illustrate the importance of the current loading on the mooring line, *i.e.* on the chain segments and on the Kevlar rope, computations for two alternative current profiles have been performed. A constant current is assumed from the free surface and down to a given water depth D_{Curr}, while the current is set equal to zero for larger depths. Computations for D_{Curr} =100m and 20m are performed. In the latter case, the current only acts on the buoy itself, *i.e.* as in the computations by Genimar. The results for the horizontal offset, the vertical setdown and the mean tilt angle are presented in Figure 22-Figure 24. It can be noted that current force on the mooring line gives significant contributions to the translatory offsets, while the tilt angle is nearly unaffected by it. For D_{Curr}=20m, the results for the horizontal offset and the tilt obtained by RIFLEX nearly coincide with the calculations performed by Genimar. Since Genimar does not account for the setdown due to the horizontal displacement of the buoy, the setdown results differ. These results give confidence in the present model, and it is believed that it provides good results for the overall global behavior of the buoy.

In Figure 24 the mean tilt angle for the altered buoy design, where the vertical distance from the fairlead to the sphere is increased by 1 meter, is included. This shows that by lowering the fairlead relative to the center of buoyancy, the mean tilt angle of the buoy in current will decrease.

7. STRUCTURAL ASSESSMENT OF CURRENT DESIGN

7.1 Kevlar cable

The forces in the Kevlar cable is calculated as part of the above hydrodynamic analyses of the buoy. This is done by non-linear, time-domain stochastic dynamic analyses, with integration of hydrodynamic forces to the instantaneous wet surface. A three-hour simulation of sea state no 3 gives the following forces in the cable:

Maximum tension N_{max} = 33 kN, or roughly 3.3 tonnes force
Minimum tension N_{min} = 11 kN

The Kevlar cable has a capacity of some 90 kN, which should give sufficient reserves. Furthermore, the mooring line will be kept under constant tension, which is important for a Kevlar cable.

7.2 Carbon fibre part of the buoy

The forces in the upper part of the buoy are also extracted from the hydrodynamic analyses of the buoy. A three-hour simulation of sea state no 3 gives the following maximum shear forces at the connection between the carbon fibre part and the aluminium part

Shear force Q = 1.2 kN, or roughly 0.12 tonnes horizontal force
Bending moment M = 13.4 kNm
Force resultant acting a = 11.5 meters above the intersection between carbon fibre and aluminium

Rivoyre Ingeniere has performed finite element analyses of the carbon fibre part of the buoy. A beam model of the carbon fibre trusswork has been established, and analysed under a lateral load of 1 tonne (10 kN), acting on the tip of the trusswork. A series of statical, linear analyses have been performed, concluding that the top part of the buoy has a capacity in the order of 20 kN with respect to lateral loading at the top of the mast.

This indicates that the carbon fibre part of the mast has significant reserve capacity.

It should however be noted that no separate evaluation has been performed of the strength of the connections between diagonals and verticals in the carbon structure.

7.3 Aluminium trusswork

A three-hour simulation of sea state no 3 gives the following maximum shear forces in the aluminium trusswork:

Shear force	Q = 1.3 kN, or roughly 0.13 tonnes horizontal force
Bending moment	M = 16.3 kNm
Force resultant acting	a = 12.5 meters above the centre of the sphere

A small FE model of the aluminium trusswork has been established to determine the capacity of the lover part of the mast. A non-linear quasi-static analysis has been performed, with the aluminium truss subjected to 4 kN (400 kg) vertical load and a horizontal load of 1.3 kN acting at the top of the aluminium part, and a bending moment representing the remaining moment arm above the top of the aluminium mast. Model and analysis results are shown in Figure 26.

For this loading, the aluminium starts to yield at 21 kN, and reaches its ultimate collapse capacity of 30 kN. This is significantly more than the required capacity.

It should again be noted that the brace/chord connections of the aluminium structures has not been investigated in detail, and that only this loadcase has been investigated for collapse.

7.4 Connection between sphere and aluminium tubes

To determine the order of magnitude of the stresses in the aluminium skin, a local FE model has been established to replicate main characteristics of the sphere / tube intersections. Since detailed information about the construction of the sphere is not available, a simplified FE model is made, representing an aluminium tube intersecting a flat plate with equally spaces longitudinal and transverse stiffeners. This is of course a severe simplification compared to the real structure. It should however give information about the main load-carrying mechanisms, and should provide the order of magnitude for the stresses in the connection. The model is shown in Figure 27. Figure 27c shows the axis system used as reference for discussion of the results, i.e. tangential to the sphere ("*x*-direction") and radial to the sphere (*"y*-direction").

Figure 28 - Figure 30 illustrate the stress distributions in the aluminium skin under various loading conditions: Figure 28 shows stresses in the plate when the tube is exposed to a unit axial load. The horizontal axis indicates locations on the plate, and the vertical axis indicates plate stress per kN axial load. Figure 29 shows stresses in the plate when the top of the tube is given a unit radial displacement. The horizontal axis indicates locations on the plate, and the vertical axis indicates plate stress per 1 mm displacement. Figure 30 shows the stresses in the plate when the top of the tube is given a unit radial displacement. Same axis definitions as Figure 29.

Even if both the FE model and the simplification in geometry are quite coarse, the analyses indicate a significant concentration of stresses in the tube/skin intersection, and very high stresses

even for small flexural deformations of the aluminium tube. 1 mm radial deflection of the top of the tubes in Figure 29 generates stresses above the yield strength of the aluminium skin, and 1 mm tangential deflection of the tube in Figure 30 generates stresses in the order of half the yield strength.

The relative deformations between different elevations in the aluminium truss are estimated from the FE model of the aluminium trusswork. Lateral deformations at different elevations in the aluminium mast are listed in Table 1, compared to the deflections at centre of the sphere. The right-hand column lists standard deviation of deformations, for fatigue assessment.

Table 1 Relative deflections of the aluminium mast, i.e. lateral deformations at different elevations in the aluminium mast compared to the centre of the sphere

	Deformations in storm situation (Seastate 3) [mm]	**Deformations in regular conditions / fatigue (Seastate 1) [mm]**
Top of aluminium part	5-7	2.5
Lowest horizontal in the aluminium mast	1	0.5
Top of sphere	~0.2	~0.1

According to Figure 29 and Figure 30, this corresponds to standard deviations for plate stress in the order of σ = 15-30 MPa, depending on whether the loading is assumed tangential or radial to the sphere.

This should be compared to the fatigue capacity of the tube/skin connection, as given by the SN-curves in Eurocode 9 "Design of Aluminium Structures". Max allowable stress range for the plate stresses are listed in Table 2, together with the corresponding standard deviation of stresses. Details are listed in Appendix E.

Table 2 Estimated fatigue life for different stress ranges

Lifetime	**Number of cycles**	**Max. allowed stress range, s_{eq} [MPa]**	**Corresponding standard deviation of stresses, σ [MPa]**
1 month	$3.7 \cdot 10^5$	31	10
3 months	$1.1 \cdot 10^6$	22	7
6 months	$2.3 \cdot 10^6$	17	5.6
1 year	$4.5 \cdot 10^6$	14	4.4

This means that the tube/sphere connection is likely to be exposed to higher stresses than it can take, and that it is unlikely to survive long periods in the sea.

Since the return period for Seastate 1 is not known, it is hard to determine exactly what fatigue life this corresponds to (how many months at sea). The analyses are based on a number of crude simplifications, and should be used with caution. However, the analyses clearly indicate the tube/sphere intersection as a critical detail where potentially very high stresses can be generated. The analyses also indicate that the order of magnitude of these stresses can be in a range compatible with failure of the structure after relatively few months at sea.

7.5 Workmanship

One remaining structural cause for the buoy taking in water could of course be poor workmanship and gross defects in the welds, e.g. in the tube/skin intersections. However, there is nothing in the information given to MARINTEK that would substantiate such a claim.

8. ALTERNATIVE SOLUTIONS

8.1 General

The present work has identified the following areas that should be evaluated in the development of the new design:

- The present design for the top mast (carbon fibre and instrumentations) seems well suited for the purpose, and need not be changed. However, a less costly material than carbon fibre can be used without compromising buoy stability, provided the lower part of the buoy is modified to maintain the hydrostatic stiffness, e.g. by increasing the distance from fairlead to the centre of the buoy.
- The buoyancy body could with benefit be made in synthetic foam (e.g. polyurethane) with a skin in fibre-reinforced epoxy, rotationally moulded polyethylene or cast/sprayed polyurethane elastomer. Several commercial buoyancy products are available, which could easily be adapted to the present purpose. See e.g. Figure 31 to Figure 33.
- The lower part of the mast (aluminium part) should be re-designed to fit the new buoyancy body or bodies.
- Polyester rope should be considered for the mooring line instead of Kevlar.

8.2 Mooring line

Failure of the mooring line has happened in two occasions in the present project:

- The mooring line of the initial deployment was lost, possibly because the temporary buoyancy installed was not sufficient to ensure that the Kevlar cable was kept under tension in all situations.
- The entire buoy was lost during salvage operations because the Kevlar cable broke.

A reason for choosing Kevlar can be to establish a stiff enough system for the heave eigen period to fall below the region of wave excitation. For the present case, however, this has not been successful. On the contrary, the heave period ends up in a region where large wave loads can be expected.

Alternatively, one may try to increase the heave period to a value above periods of significant excitation. Polyester rope might then be a better choice for the mooring line. Firstly, the price of polyester is much lower, and secondly it is less sensitive to compression and bending which diminishes the chance of damaging the rope during handling. Moreover, a softer mooring line can increase the heave eigen period to a region of less wave excitation. (A 50% reduction in axial stiffness will result in a 41% increase in the heave eigen period (from 9.0s to 12.7s).) This may also increase the weather window for operation of the buoy.

Increasing the vertical distance from the fairlead to the centre of buoyancy will reduce the mean tilt angles. One should however be careful so that buoy does not experience significant wave excitation for the pitch eigen period.

8.3 Buoyancy body or bodies

Figure 31 to Figure 33 shows buoyancy bodies available commercially. It would seem that some of these bodies would be well suited for the present application – hydrodynamic loading will be significantly reduced at –17 meters depth compared to the conditions at the sea surface.

One might consider a single, large volume for buoyancy (much like the present design), or a solution where a series of smaller buoyancy elements are attached to the tubes in the lower part of the buoy. This is illustrated in Figure 34.

8.4 Structural detailing

Structural detailing can easily be adapted to the new buoyancy elements.

9. ASSESSMENT OF BUOY LIFETIME

MARINTEKs review of the buoy design has only identified one structural detail that can seriously affect the buoy lifetime. This is the transition of the aluminium tubes through the skin of the buoy, where abrupt change in geometry can cause significant concentration of stresses in very local areas. If such details are omitted in the future design, we see no reason why the structure should not confirm to the standards typically expected from marine and offshore structures.

Commercial polyurethane buoyancy products have proven themselves through real-life application in much worse environments than is the case for the present design, and should not be a limiting factor for the buoy lifetime.

Polyurethane mooring lines have also been used in a number of offshore applications, so far with good performance. However, a careful screening of available products and references is recommended.

A periodic diving inspection programme of the buoy structure is recommended for the first one or two years of deployment, e.g. coinciding with regular maintenance of the optical instruments. If inspections are successful (i.e. no findings), the intervals can be relaxed to yearly of bi-yearly.

Detailed calculation of fatigue life of the structural components is deemed to be outside the scope of the present contract. However, the necessary figures for such calculations can be derived from the analysis results listed in Appendix D.

10. REFERENCES

/1/ Statement of Work.
Assessment of the buoy system Boussole:
Risk evaluation and advices
Goryl Philippe & Thouvenot Eric, ESA
ESA reference ENVI-CLVL-EOAD-SW-02-0006, 14 August 2002

/2/ The Boussole Project
(1) Progress Report
(2) Analysis of the June 2002 events
(3) Plans for 2002-2004
Appendix 0 included
David Antoine, Laboratoire d'Océanographie de Villefrance
LOV note dated 5 July 2002

/3/ Bouée Support de Mesure en Mer
Pierre Guével, GENIMAR
GENIMAR Note technique G1298/BSMEM-01

/4/ Bouée Support de Mesure en Mer
Pierre Guével, GENIMAR
GENIMAR Note technique G1298/BSMEM-02

/5/ Essais en bassin d'une Bouée Support de Mesure en Mer
Rapport d'essais
Jean-Claude Dern, BGO First
BGO first report 9.8.2 006, 8 October 2002

/6/ Numerical calculations of rib-stiffened aluminium sphere exposed to 2 bars external pressure
Pascal Dargent, le Laboratoire de Physique et Chimie Marines, Observatoire Océanologique CNRS-INSU-UPMC
Telefax dated 28 March 2000

/7/ Projet Boussole
Structure tubulaire de bouée
Frédéric Doray, Rivoyre Ingénierie
Rivoyre Ingénierie report dated 30 May 2001

/8/ Cahier des charges pour la construction en composite carbone de la partie supérieure de la bouée CNRS pour le projet Boussole
David Antoine, LOV
Note dated 28 August 2001

/9/ Recette de la bouée Boussole.
Structure en carbone réalisée par la société Doyle Voilerie.
David Antoine, LOV
Correspondence dated 12 October 2001

/10/ Photographs of elemnts of the buoy system prior to deployment.
Some information about the construction of the aluminium prototype
Some information about the construction of the carbon composite structure
Some information about the mooring line
Scheme of the mooring line
David Antoine, LOV
Correspondence received 15 October 2002

/11/ Cronology of events prior to loss of the buoy
David Antione, LOC
Correspondence received 15 October 2002

/12/ Weight data for the buoy system:
- partie supérieure en carbone
- partie infereure en aluminium
David Antoine, LOV
EXCEL speadsheet received 16 October 2002

11. FIGURES

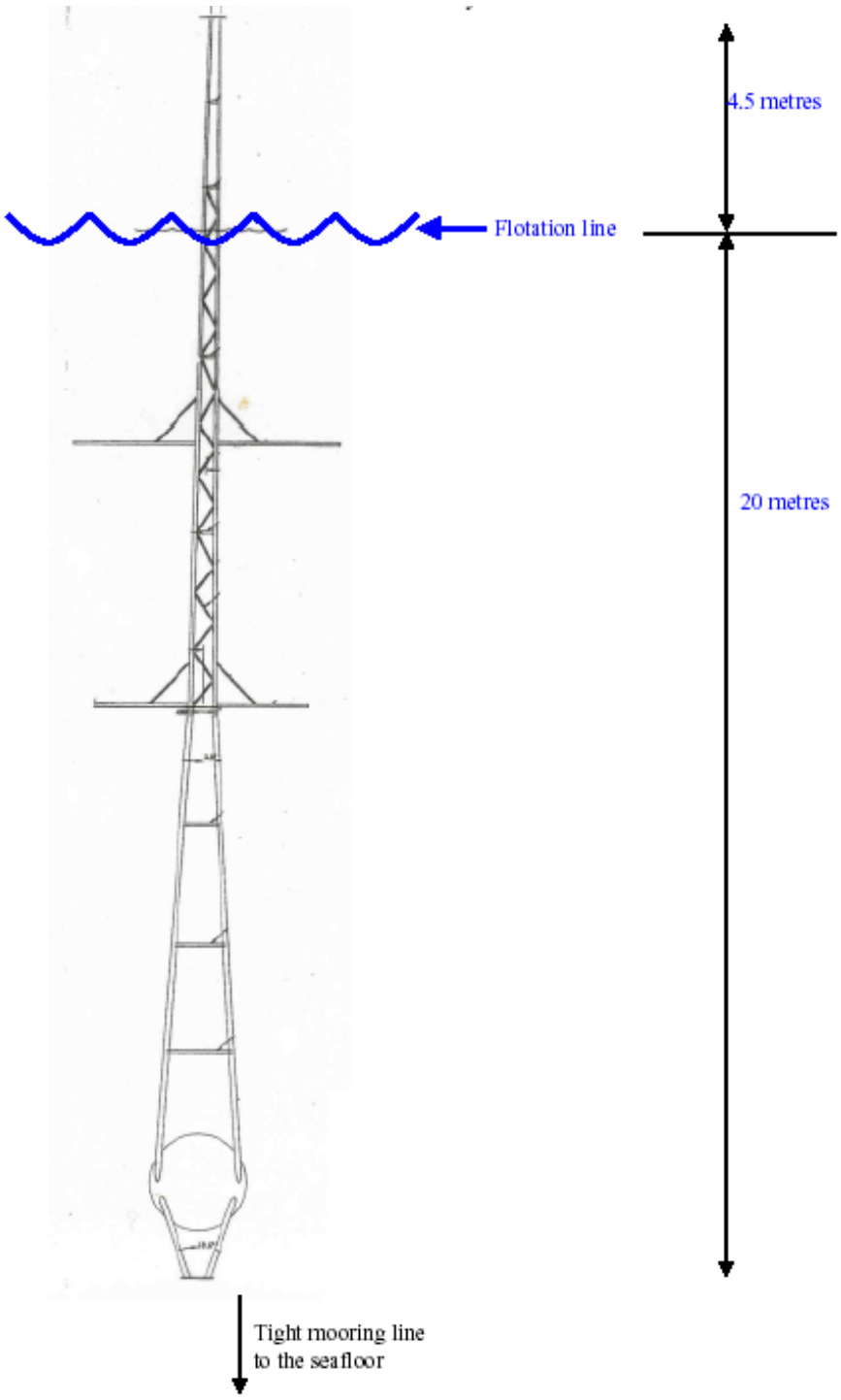

Figure 1 Overall geometry of the Boussole buoy

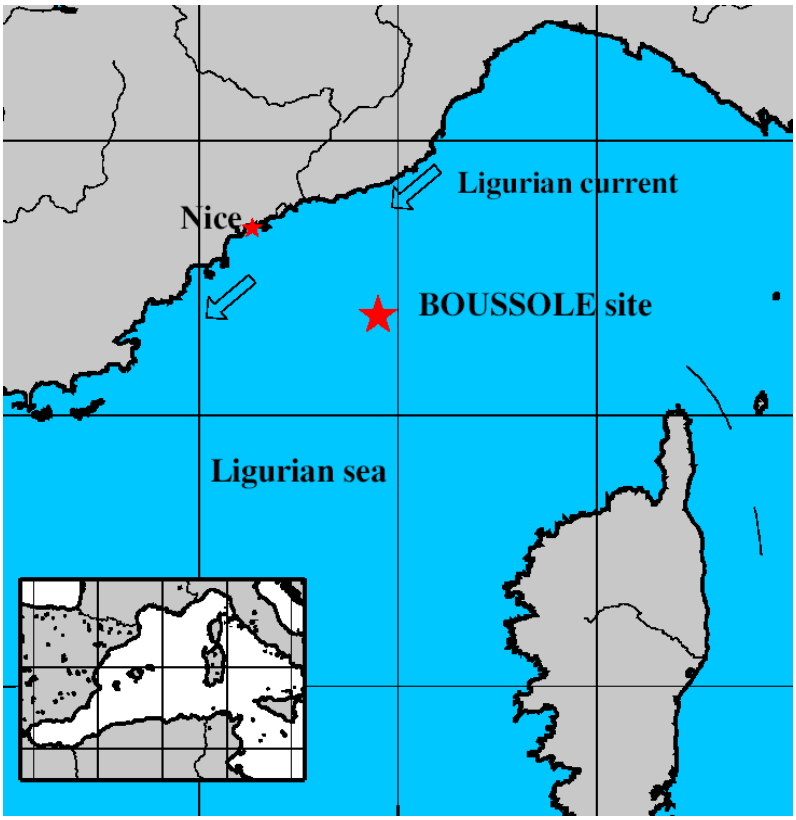

Figure 2 Location of buoy

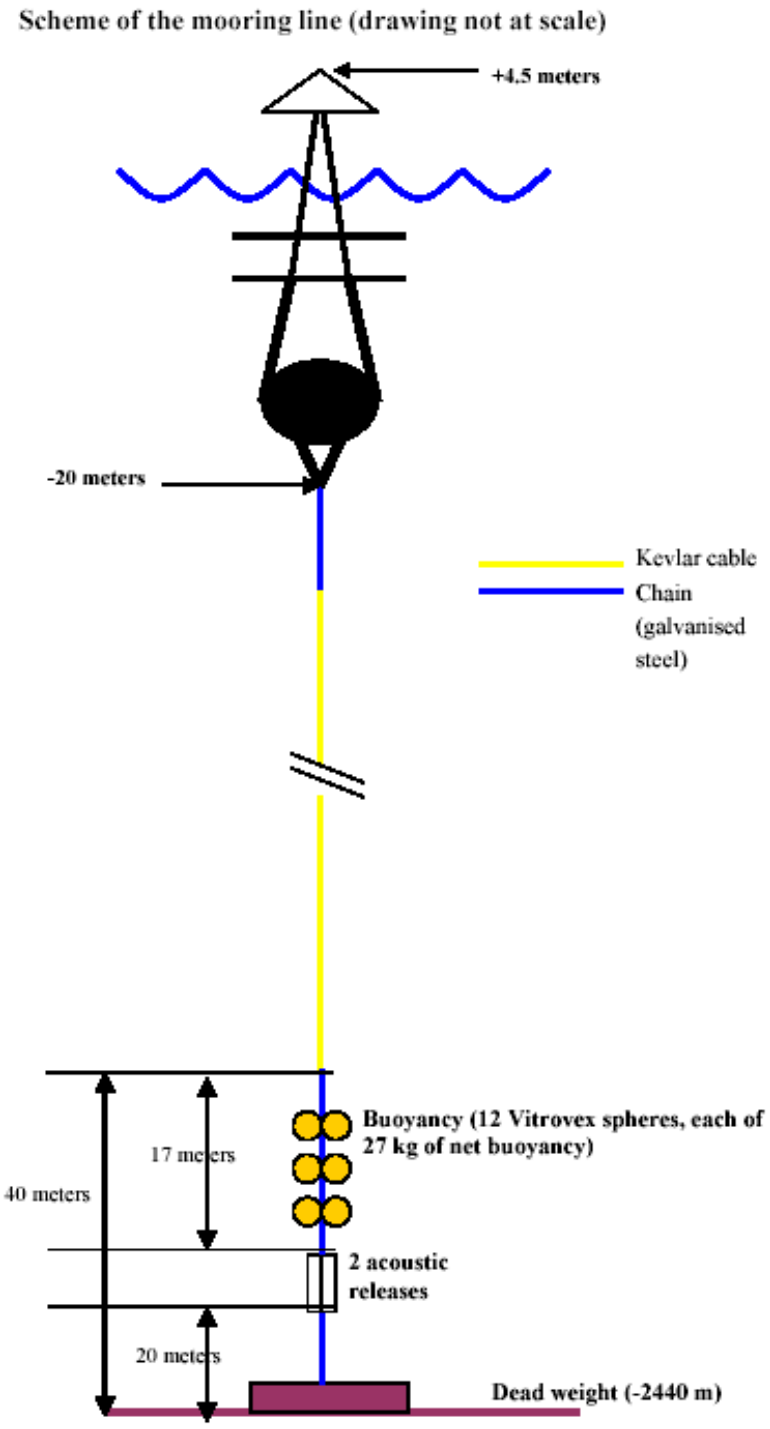

Figure 3 Mooring line schematics

Figure 4 Lower part of Buoy

Figure 5 Upper part of buoy

Figure 6 Buoy deployment.

Figure 7 Buoy at floating position

Figure 8 Kevlar cable termination

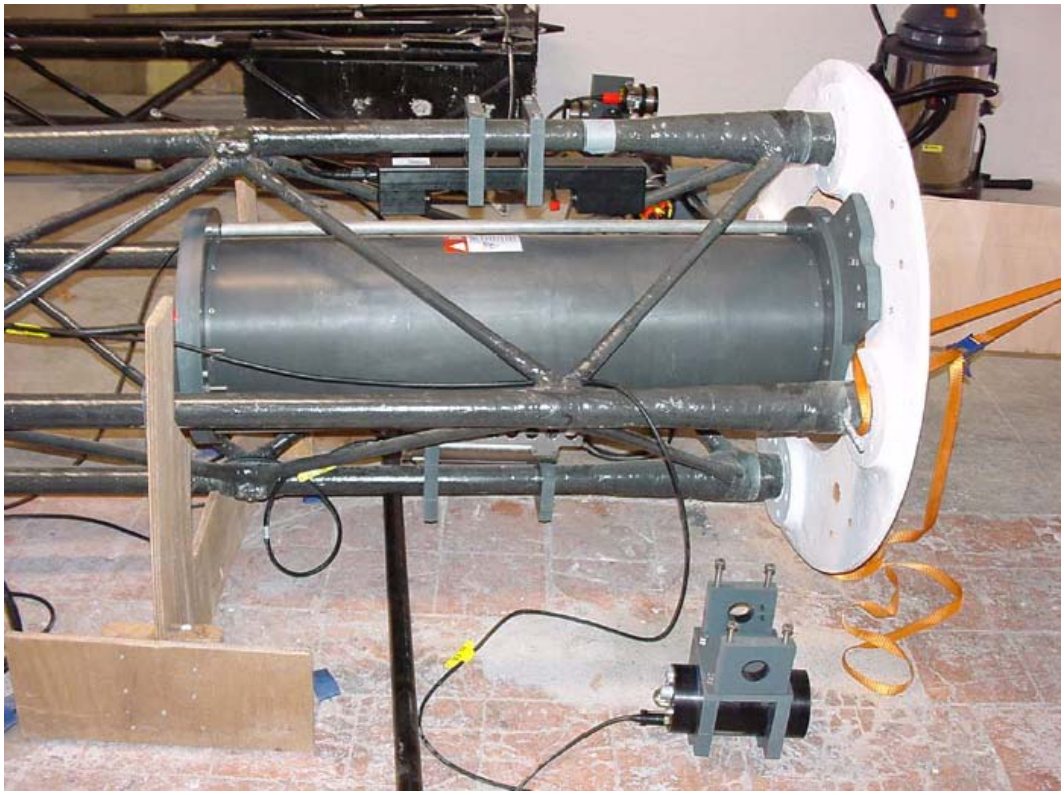

Figure 9 **Close-up of carbon composite structure (modified structure for second deployment)**

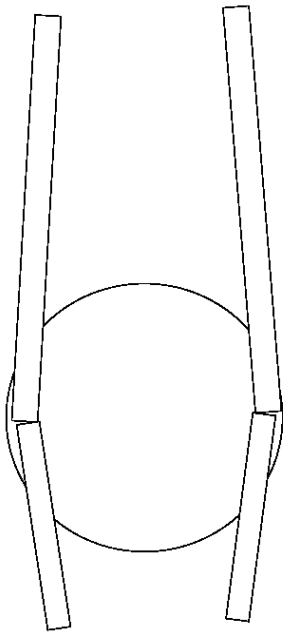

Figure 10 **Schematics of buoy design**

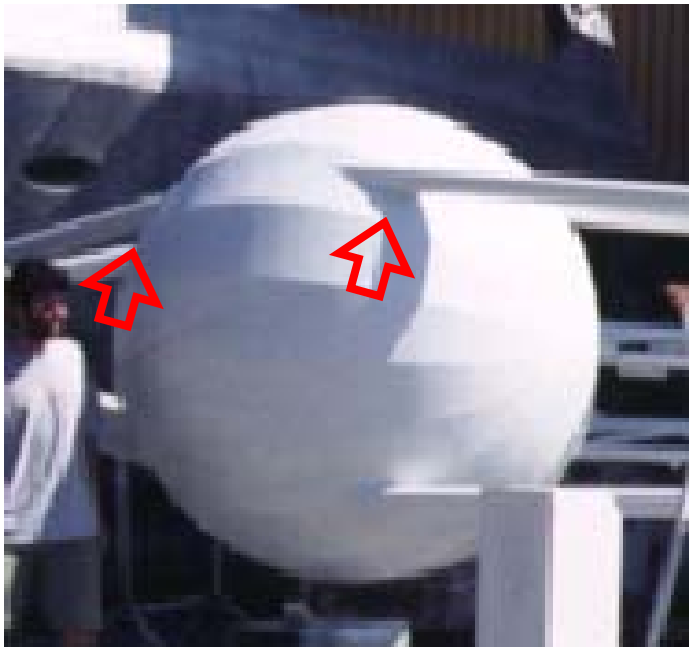

Figure 11 Critical locations

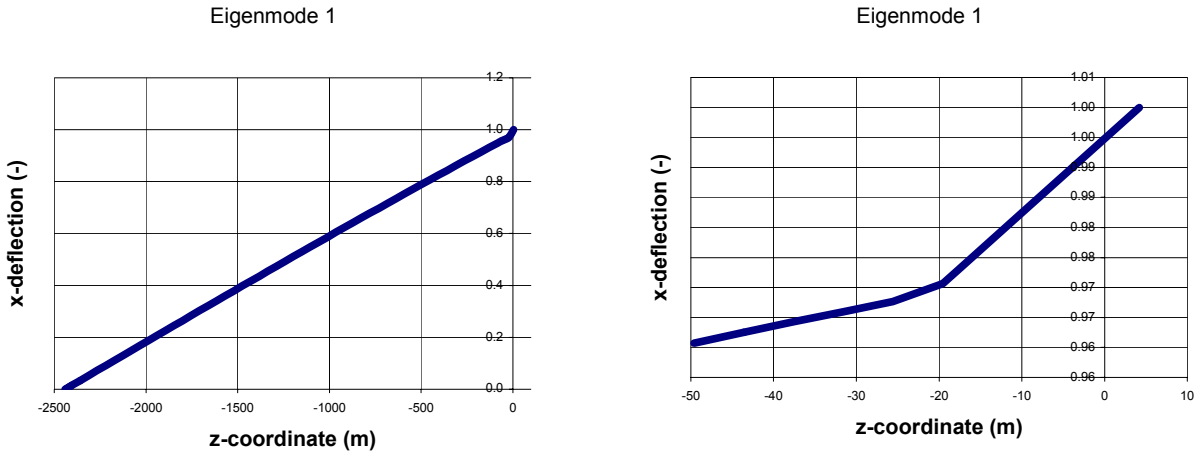

Figure 12 Shape of eigenmode 1.

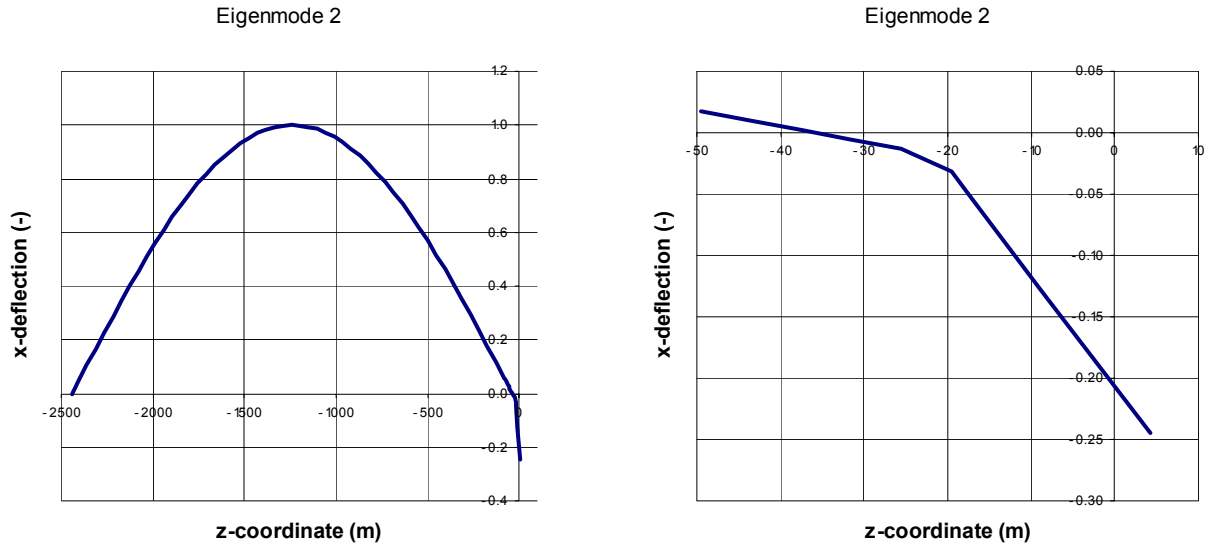

Figure 13 Shape of eigenmode 2.

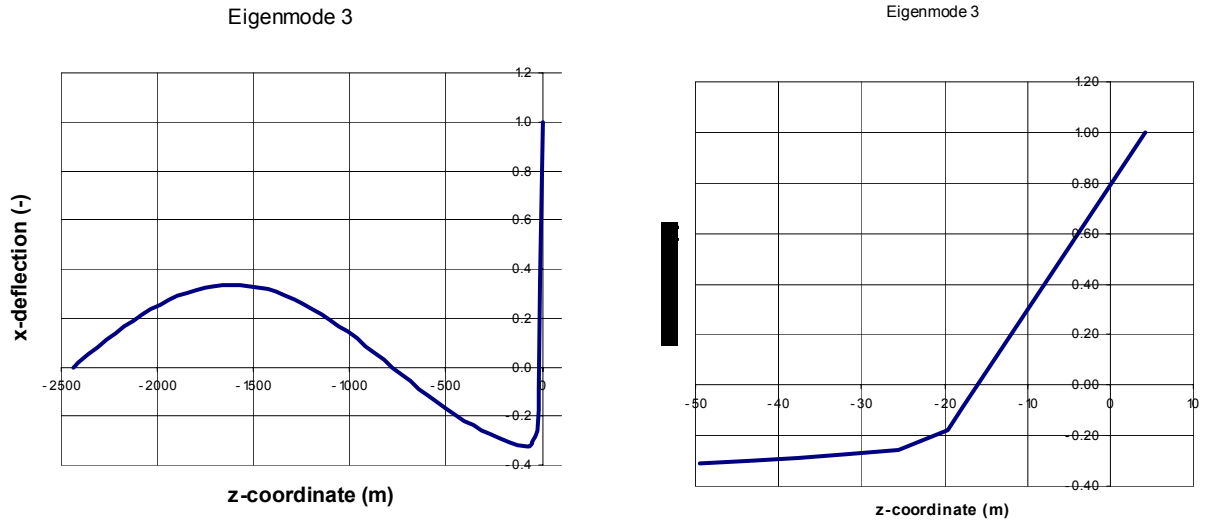

Figure 14 Shape of eigenmode 3.

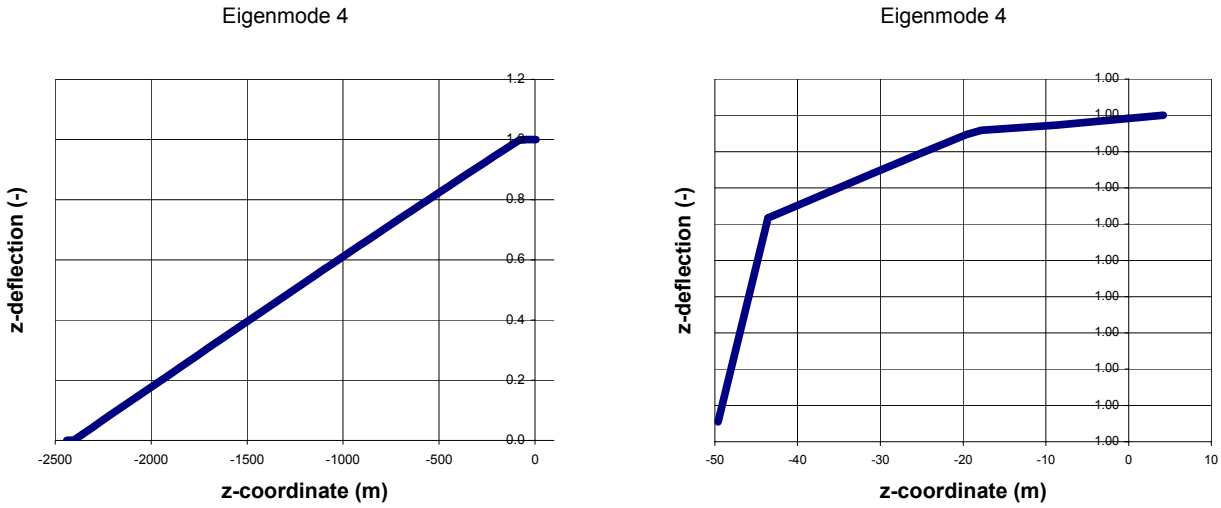

Figure 15 Shape of eigenmode 4.

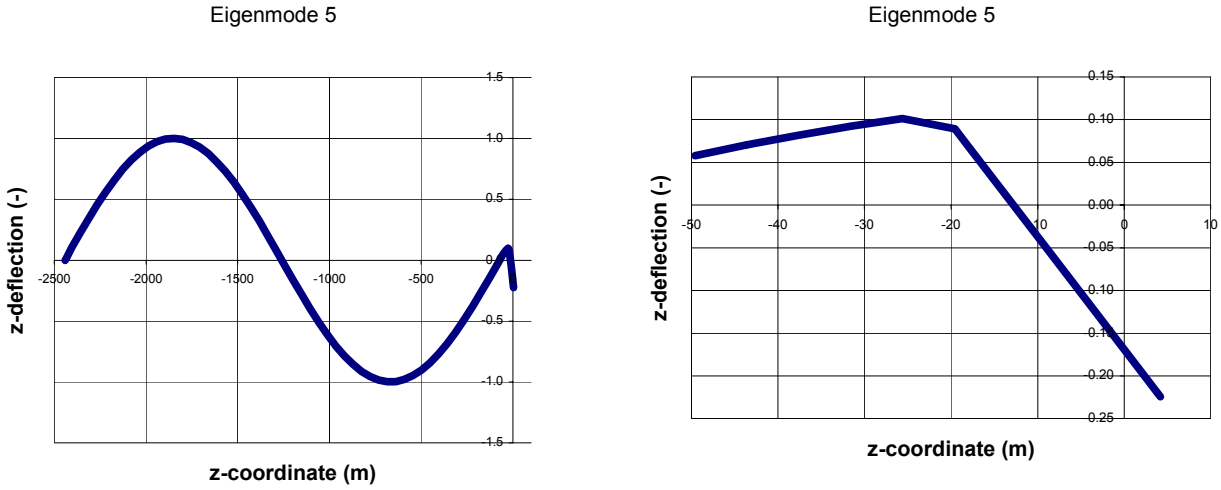

Figure 16 Shape of eigenmode 5.

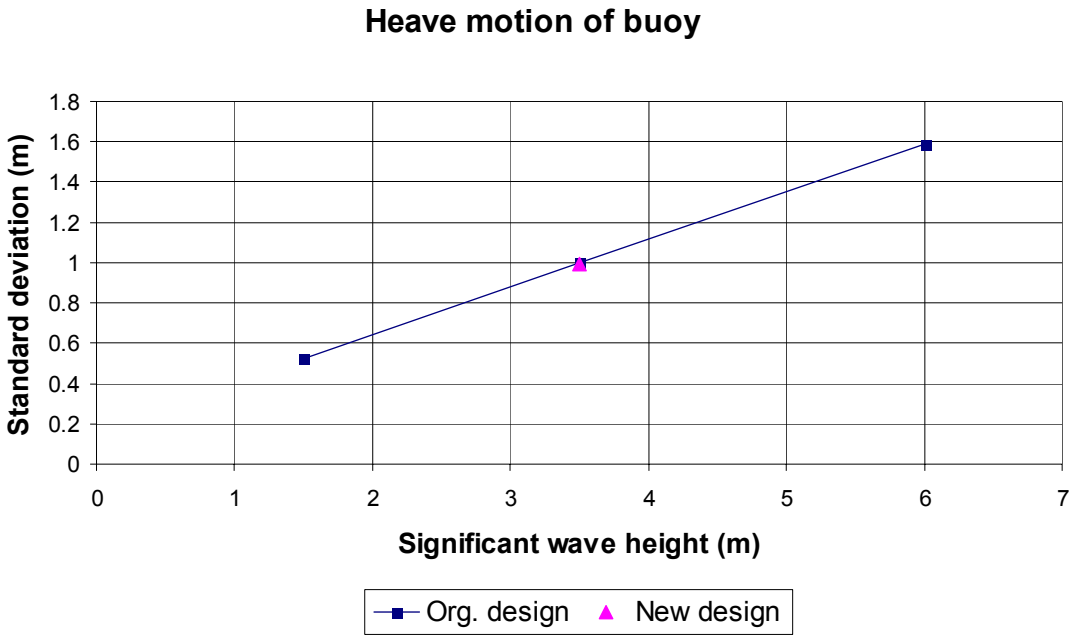

Figure 17 Standard deviation of heave motion as function of significant wave height. Note that the wave period differs for the different wave heights

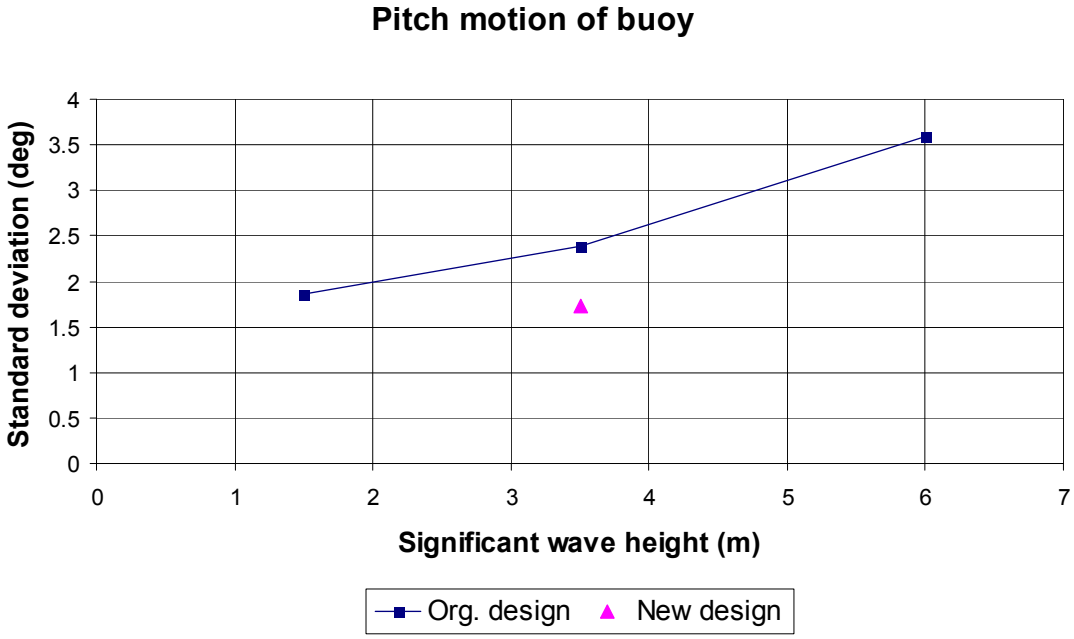

Figure 18 Standard deviation of pitch motion as function of significant wave height. Note that the wave period differs for the different wave heights

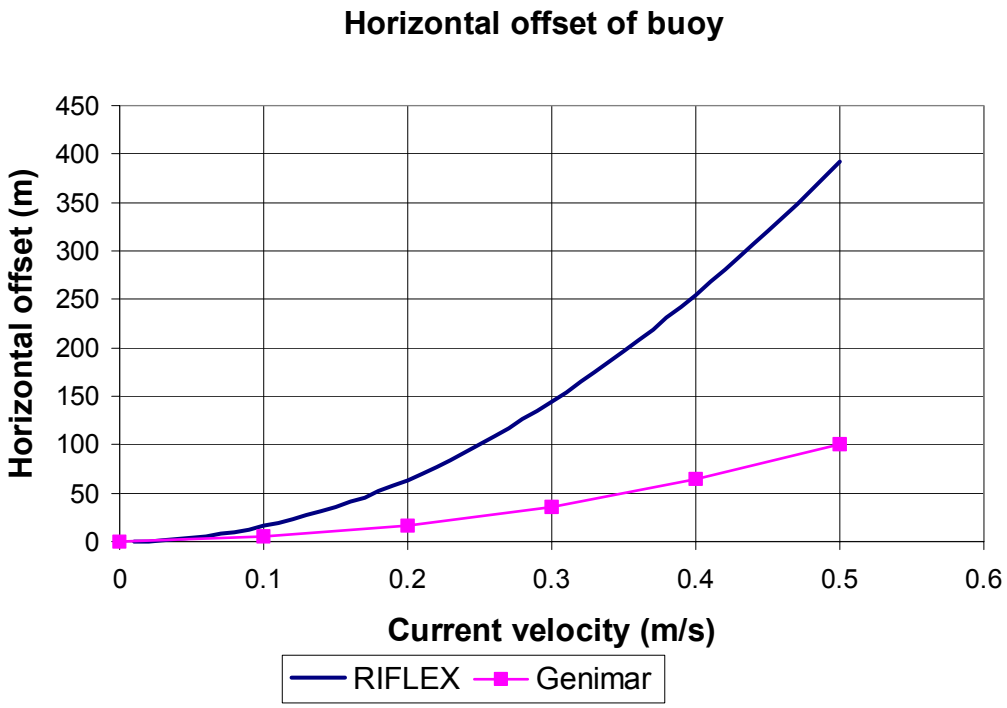

Figure 19 Horizontal offset of buoy when exposed to current only. The current velocity is assumed to be constant from the free surface to the sea floor.

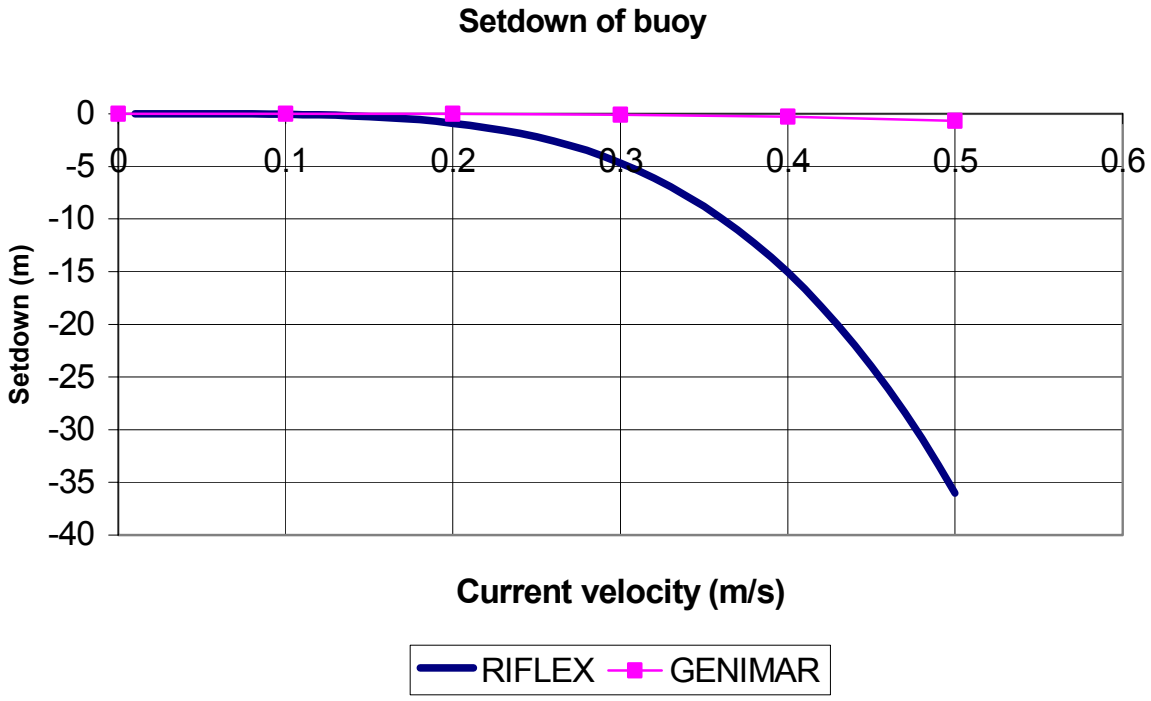

Figure 20 Setdown of buoy when exposed to current only. The current velocity is assumed to be constant from the free surface to the sea floor.

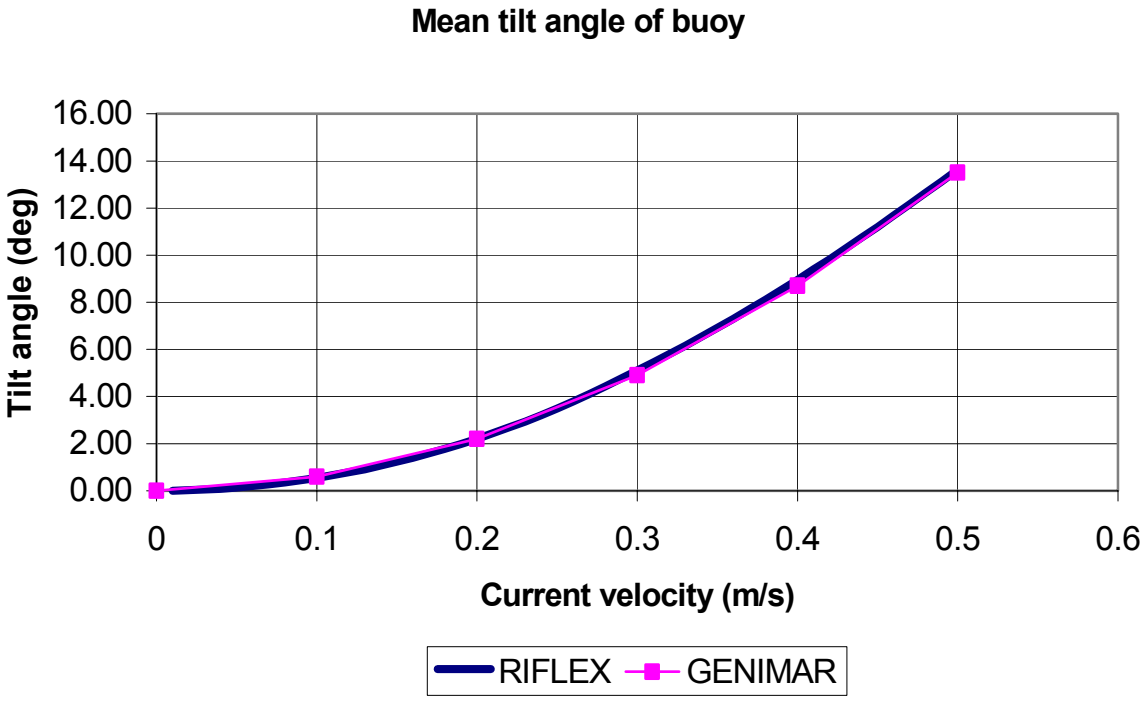

Figure 21 Mean tilt angle of buoy when exposed to current only. The current velocity is assumed to be constant from the free surface to the sea floor.

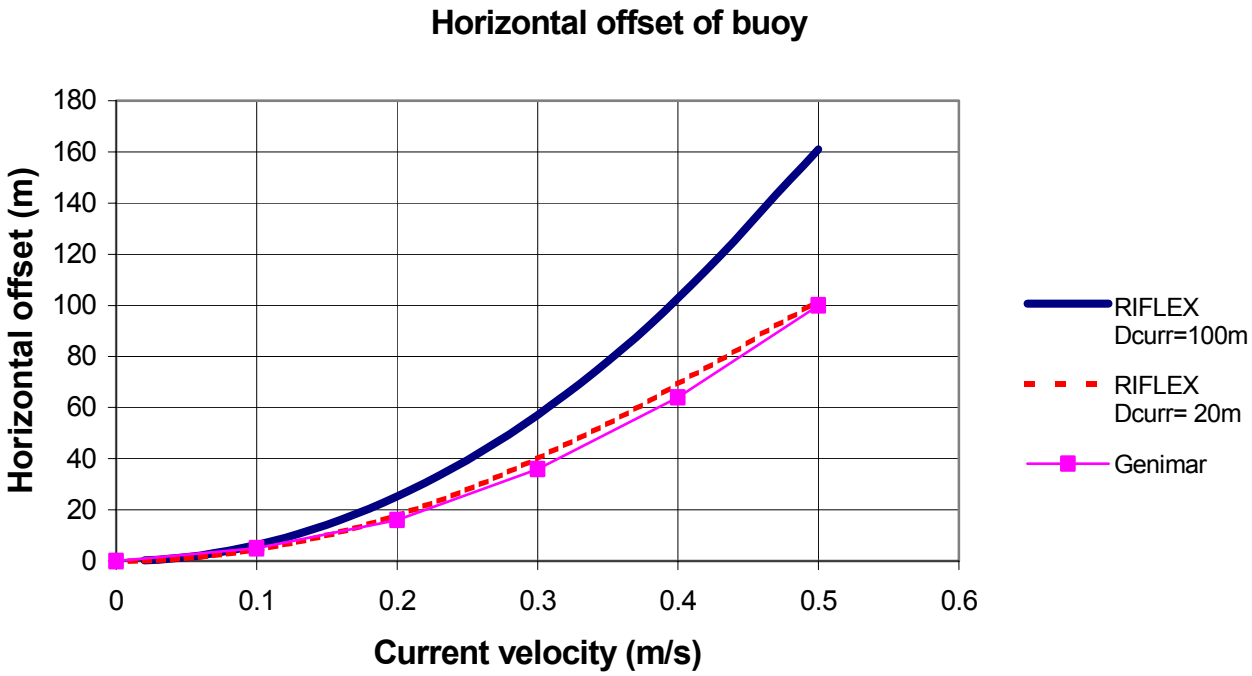

Figure 22 Horizontal offset of buoy when exposed to current only. The current velocity is assumed to be constant from the free surface to D_{Curr} and zero otherwise.

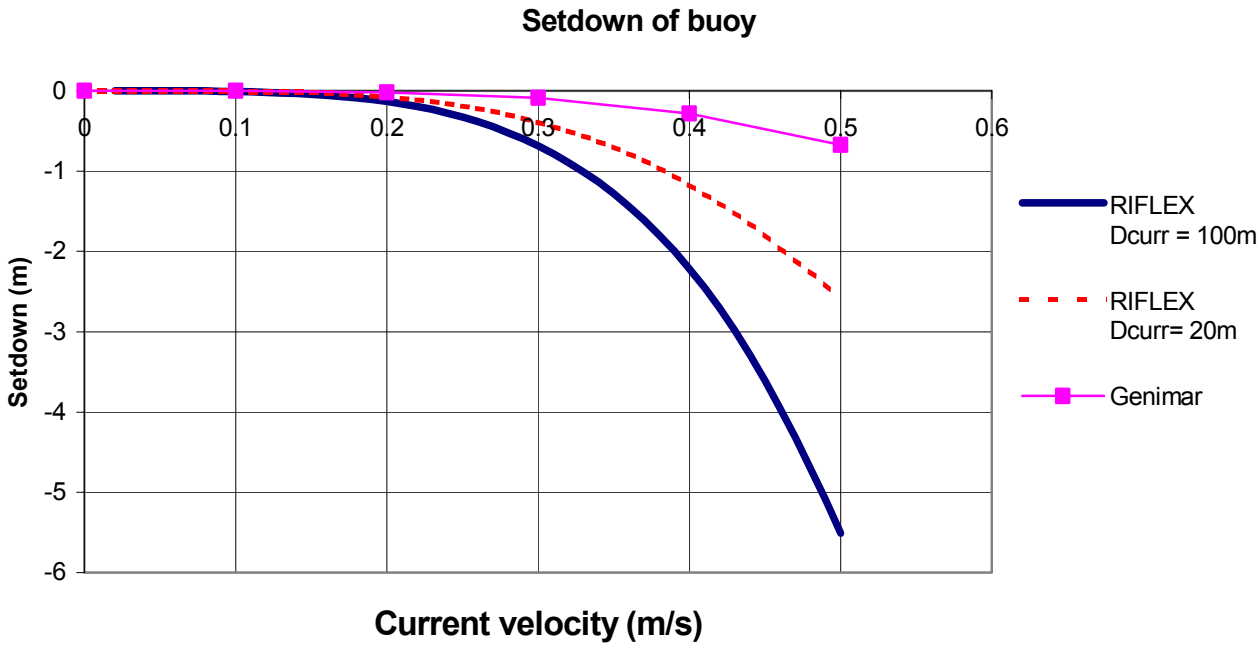

Figure 23 Setdown of buoy when exposed to current only. The current velocity is assumed to be constant from the free surface to D_{Curr} and zero otherwise.

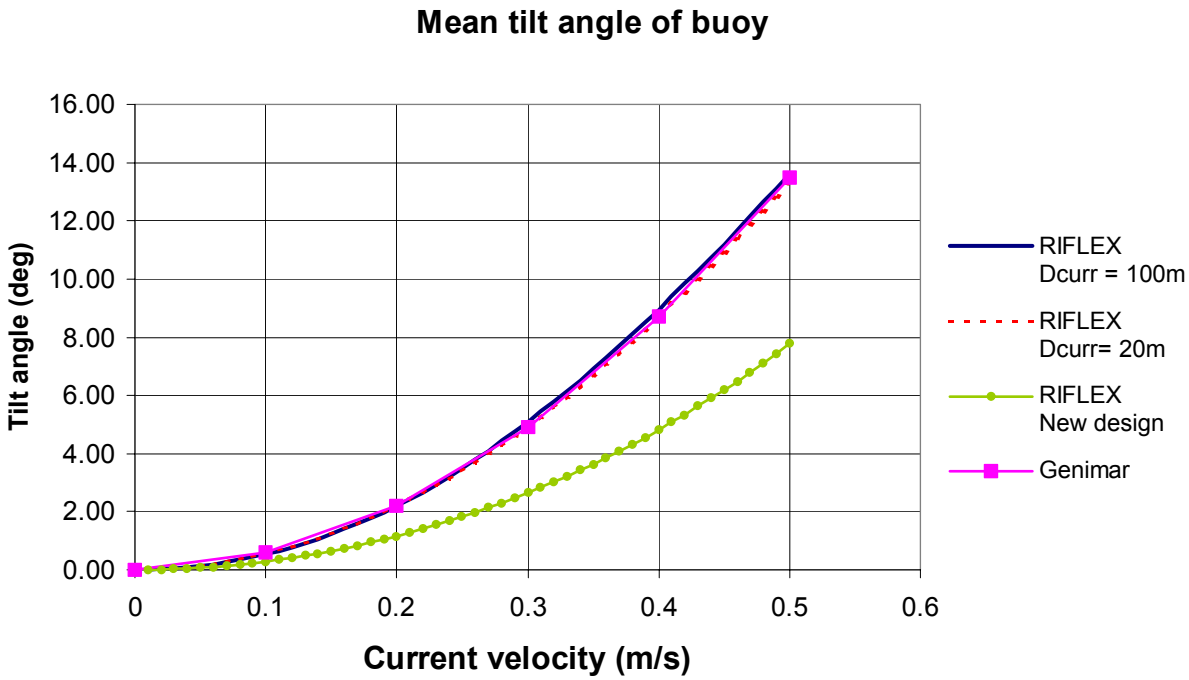

Figure 24 Mean tilt angle of buoy when exposed to current only. The current velocity is assumed to be constant from the free surface to D_{Curr} and zero otherwise.

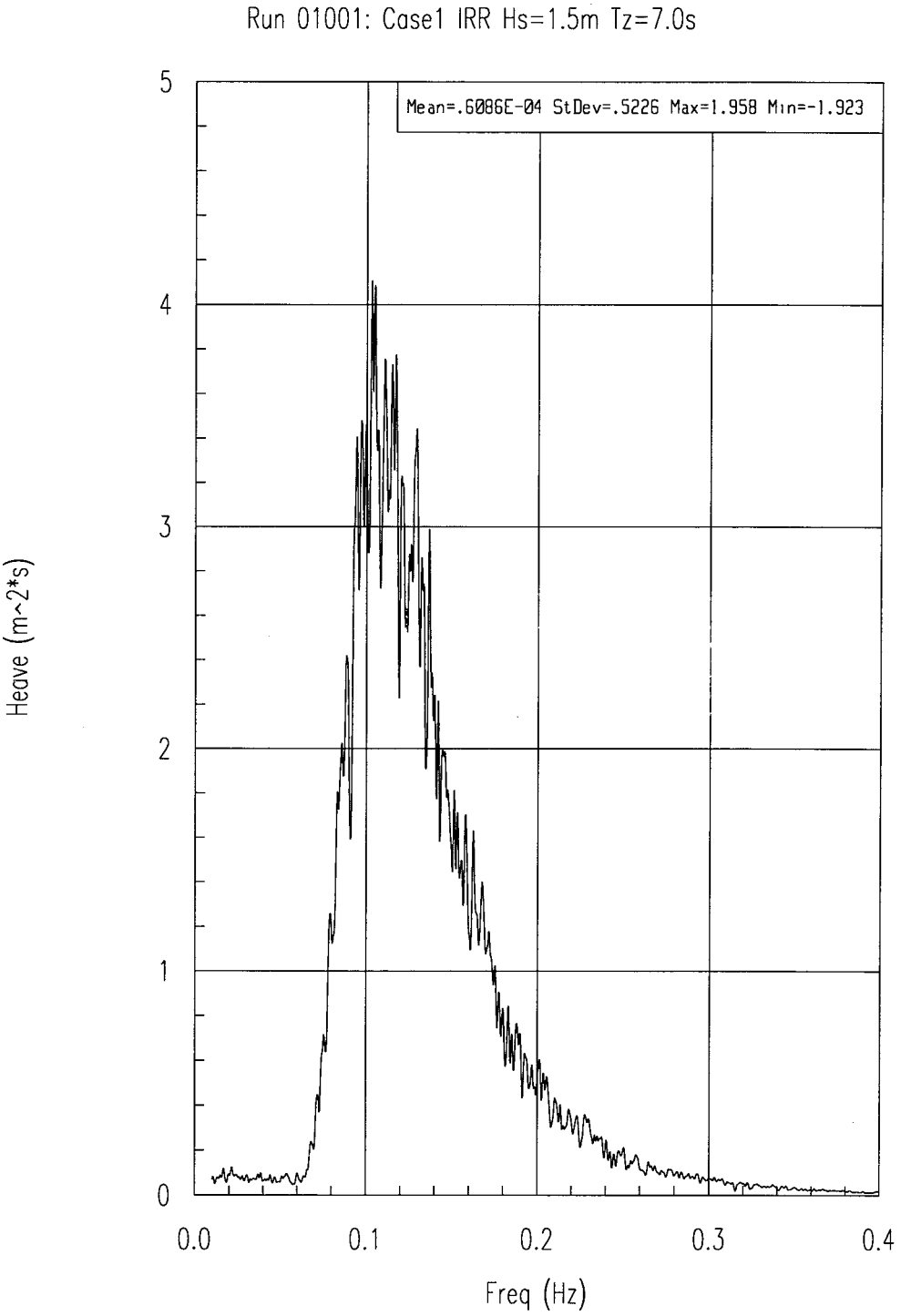

Figure 25 Spectrum for heave motion for seastate 1

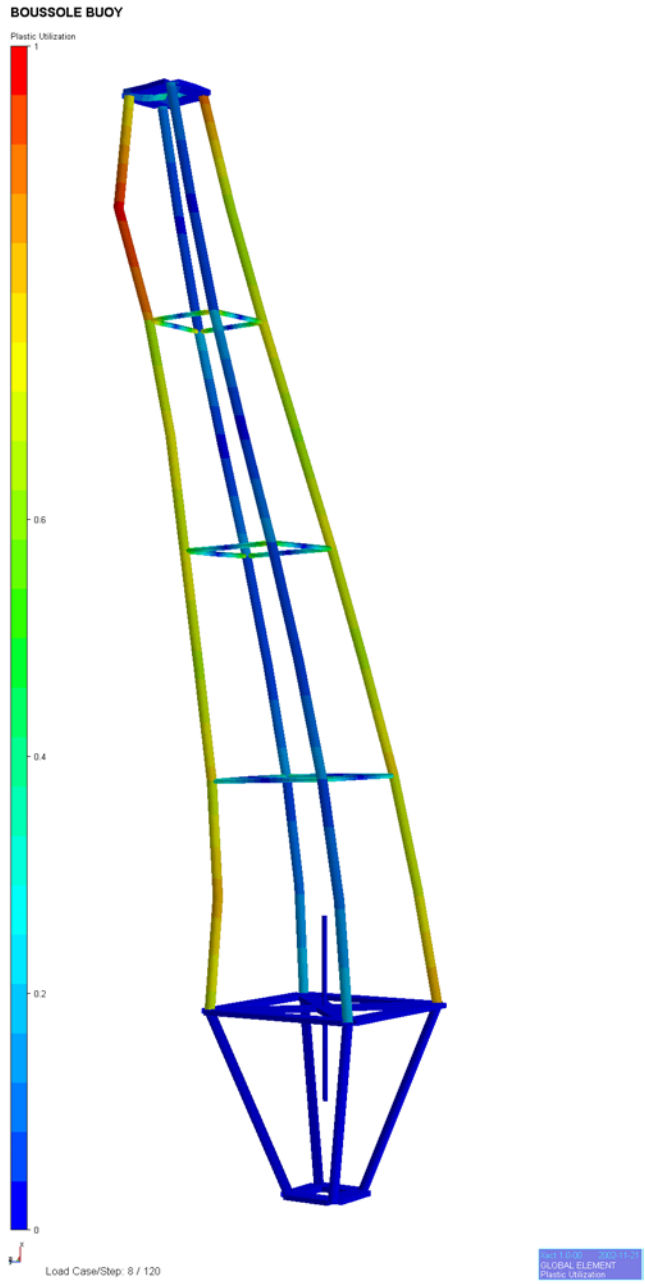

a) Deformations and plastic utilisation under a lateral load of 21 kN. This corresponds to first yield in the aluminium part.

b) Deformations and plastic utilisation under a lateral load of 30 kN. This is the collapse capacity of the aluminium part.

Figure 26 Analysis of aluminium trusswork. Deformations are exaggerated by a factor of 10

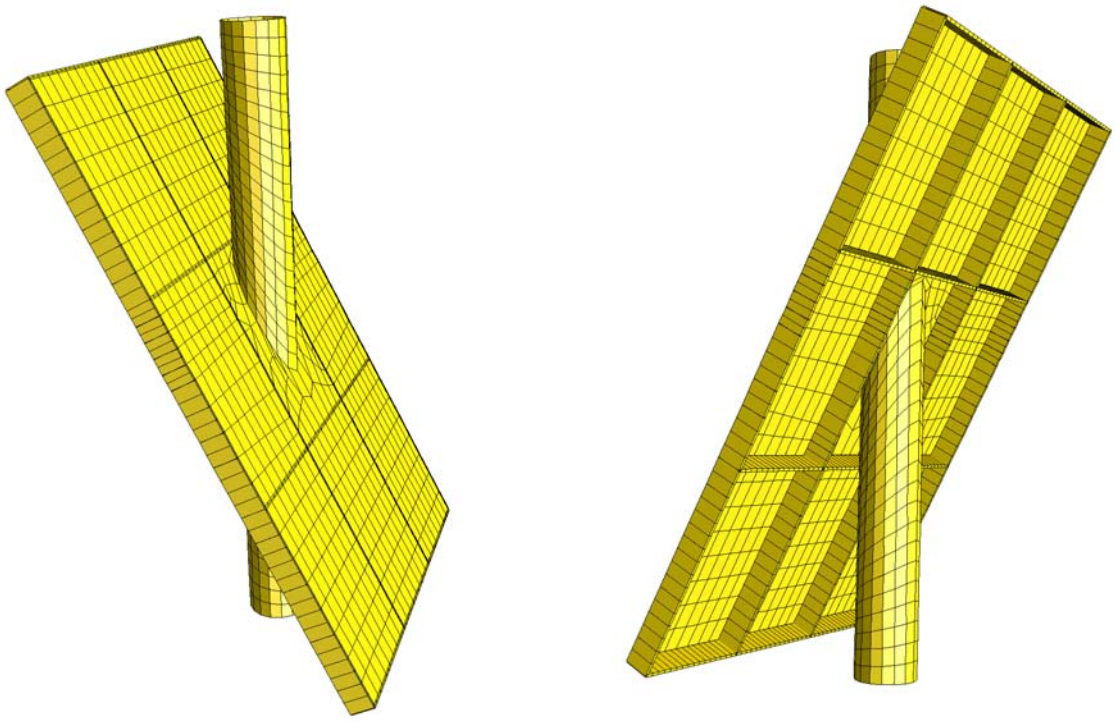

a) Outside view **b) Inside view**

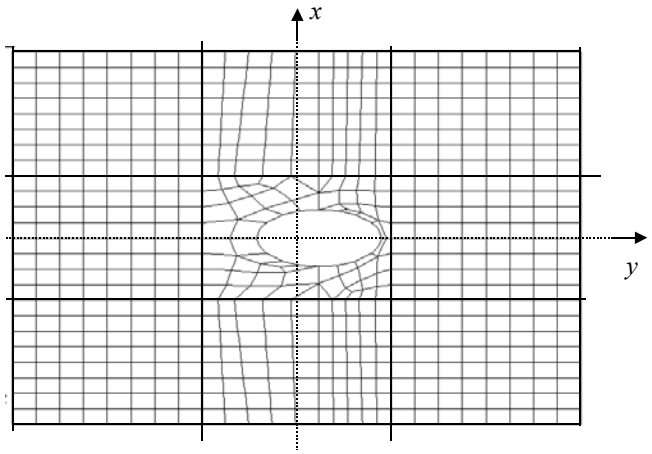

c) Axis definitions: *x* = tangential to the sphere; *y* = radial to the sphere

d) Boundary condition case 1 (BC1) **e) Boundary condition case 2 (BC2)**

Figure 27 Analysis of sphere / tube connections

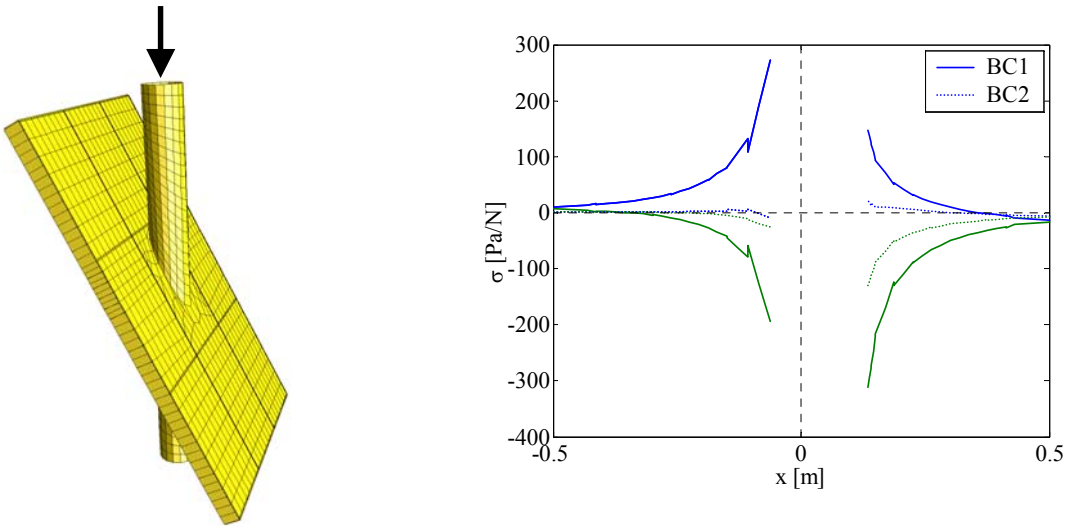

Figure 28 Stresses along the x-axis due to a unit axial force

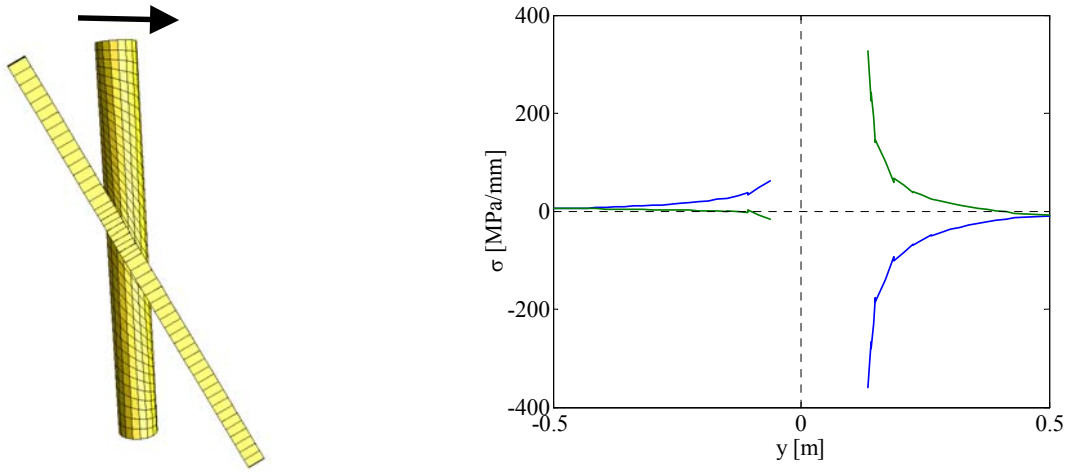

Figure 29 Stresses along the y-axis due to a unit radial displacement [MPa per mm deformation]

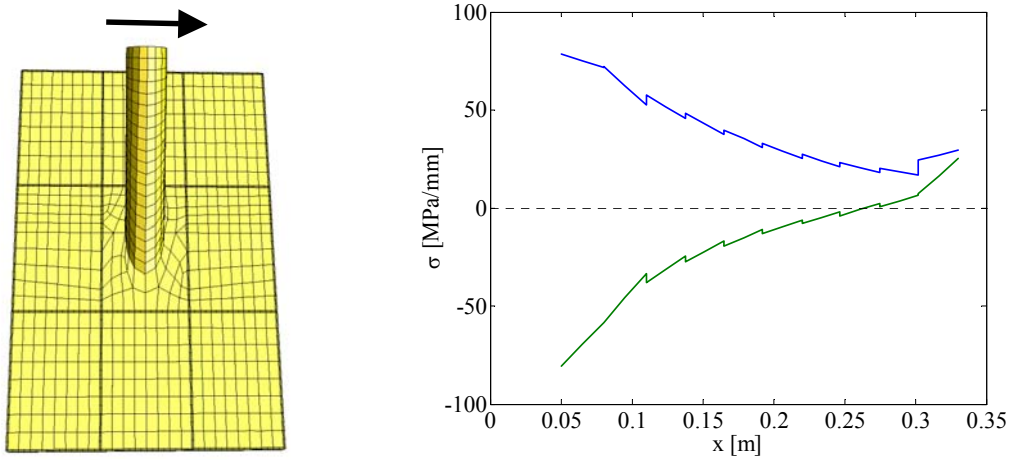

Figure 30 Stresses along the x-axis due to a tangential displacement [MPa per mm deformation]

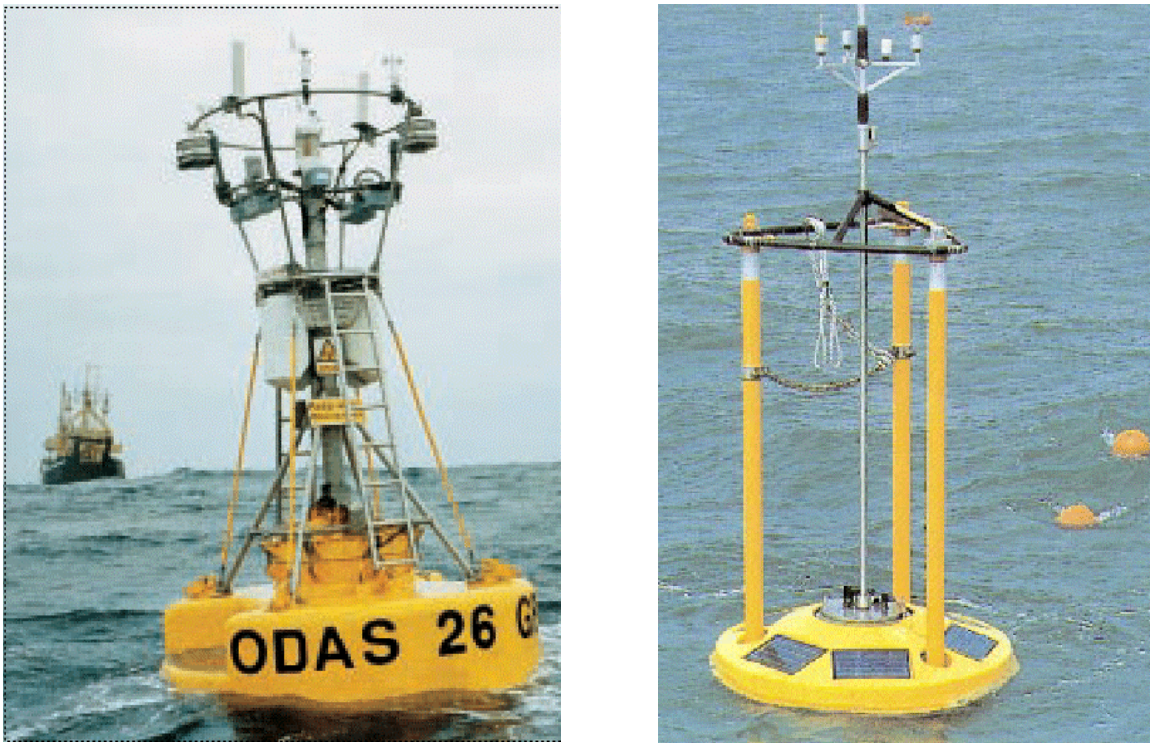

Figure 31 **Polymer buoyancy bodies for telemetric and oceanographic buoys**

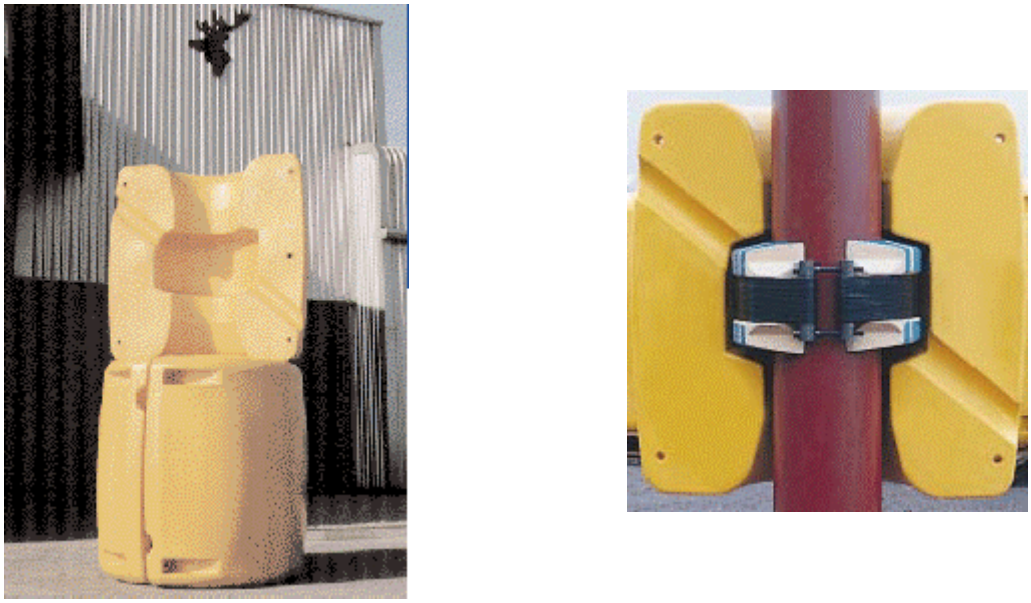

Figure 32 **Large-volume buoyancy elements for sub-sea application. To the right: specially designed clamps for easy and reliable fitting to main structure**

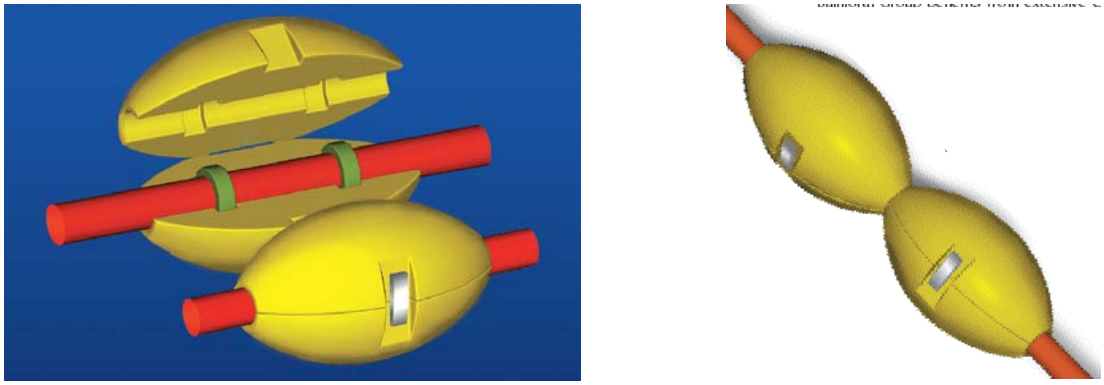

Figure 33 Buoyancy elements for distributed buoyancy. May be mounted in series.

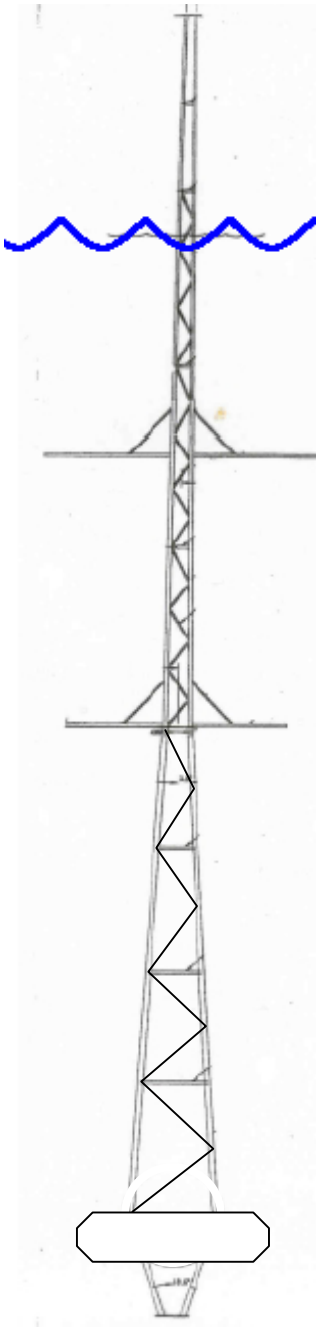

a) Aluminium sphere replaced by a single, commercial buoyancy unit made for telemetric or oceanographic buoys. Special consideration to be given to connections between aluminium tubes and buoy.

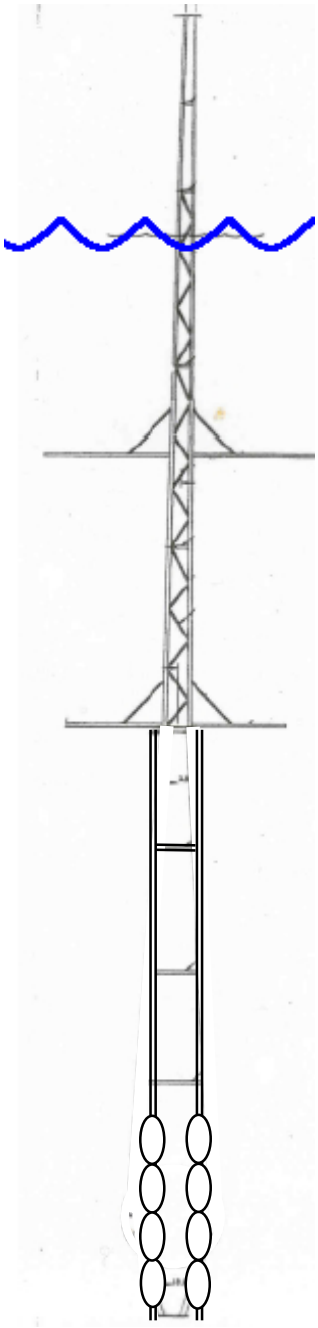

b) Aluminium sphere replaced by multiple buoyancy units clamped to the aluminium tubes.

Figure 34 Alternative buoy configurations

Appendix A SUMMARY OF BUOY DESIGN AND HISTORY

A.1 Functional requirements

The following design premises have been inferred from the documentation received from LOV:

- The instruments themselves and the platform onto which they are installed should introduce minimum perturbations in the ocean interior light field
  Shadowing in particular.
- The instruments should be as much horizontal as possible.
  An inclination of 5 degrees is indicated as the maximum tolerance
  (requirements for meteorological conditions from calm to moderate).
- The actual measurement depth should be determined with accuracy.
  Rapid vertical displacements of the instruments should be kept to a minimum.
- Performance of the buoy (motions and inclination) in cloudy conditions is of lesser importance

A.2 Design

The resulting designed is a bottom-moored buoy, stabilised by the buoyancy of an aluminium sphere (Ø 1.8 m) at -18 metres. This sphere supports a very slender trusswork structure penetrating the sea surface. Instrumentation is fixed at horizontal arms extending from the upper trusswork.

The buoy is designed in two parts. The lower part extends from –20 meters to –9 meters below the surface, and consists of the sphere and a simple tubular structure. The upper part extends from –9 meters below the surface to +4.5 meters above the surface, and hosts the instrumentation.

Aluminium structure

The aluminium structure is constructed in Al 6060 for the tubes, and Al 5083 H 111 for the skin of the sphere. Material thickness is 5 mm for tubes and skin. The 4 main tubes (outer diam. 100 mm) are connected (soldered) inside the sphere (see Figure 10). The sphere was approximated by 20 sectors of 18° each. These sectors were welded onto a space frame structure made of aluminium bars with section 8 mm by 40 mm. Other bars were placed perpendicular to these meridians (therefore like parallels on the Earth), and spaced by 30 cm. 3 tubes of outer diameter 50 mm were installed inside the sphere, one from pole to pole, and the two other ones perpendicular each one to the other, and installed in the Equator of the sphere. These tubes were connected to the 4 main tubes entering into the sphere.

Reinforcement pieces were fitted where needed, for instance at the connection between the main tubes inside the sphere.

The sphere was filled up with a 2-component foam. Waterproofness of the sphere was tested by introducing air inside the sphere at a pressure of 2 bars, and checking that the pressure was remaining stable during a full night. The whole structure was at the end covered with an epoxy primer, one layer of plastoline coating, one layer of rubber-based paint, and one black antifouling coat. The weight in air of this structure was 580 kg at the end

Carbon composite structure

The upper part of the mast was redesigned in carbone composite for the second deployment of the buoy. This part was constructed in carbon fibre tubes of diameter 44 to 55 mm. Each of the 4 main tubes was covered by a glass fibre sheath, in order to improve the resistance to local impacts. Assembly of these tubes was made with epoxy resin, and using carbon wires as well as carbon tissues with several layers of parallel fibres, each one perpendicular to the other. Figure 9 shows with some details the way tubes are assembled. The full structure, once totally assembled, was cured for 12 hours at a temperature of 65°C.

The weight in air of this structure was 130 kg at the end. The weight in air of the instrumentation installed on this structure was 250 kg (including the buoy cap structure and equipment). The total buoyancy of all the instrumentation was about 180 kg.

Mooring line

The mooring line is composed of the following elements, from the sea floor to the buoy (see Figure 3):

- A dead weight, made of a pyramidal steel structure, filled up with concrete (weight in water is 5.5 tons)
- 20 meters of chain (galvanised steel)
- A system made of 2 acoustic releases mounted in parallel (each one with a 5.5 tons capability). The system has been built by the OCEANOR/Mors company.
- 15 meters of chain, equipped with 12 spheres, each of 27 kg of buoyancy.
- A Kevlar cable (fully parallel Kevlar fibres gained into polyurethane, resistance 9 tons)
- Titanium termination at each end of the cable (see Figure 8). The chain is directly connected to that termination, without using a shackle.
- Some meters of chain (this is the mooring piece that is used at the end to fine-tune the system so that the floatation line is exactly at the desired level).
- A big shackle, linking the chain and the buoy.

A.3 Initial Deployment

The full scale "beta version" was built in spring 2000, and deployed on site for 3 months (20 of July to 20 of October, 2000).

- From mid-September to the end of the deployment, the conditions were quite rough (mean swells up to 4 meters, which mean peaks at least at 5 metres).
- Until mid September, the periods where the buoy was inclined at angles larger than 5 degrees were small.
- Oscillations were observed, which were said to match the inertial period of the ocean at the latitude of the site. I.e. oscillations are due to oscillations of the water masses after the wind stress is relaxed.

The initial deployment showed somewhat too large pitch motions in waves higher than about 2 metres, which reduced the percentage of time for which the requirements in terms of inclination is satisfied.

A.4 Modifications

It was decided to introduce slight modifications in the design and construction of the buoy before the second deployment. In order to reduce the pitch motions, following changes were introduced:

- The sphere was sphere lifted to -17 metres depth instead of -18 metres. Thus, the distance from the centre of the sphere to the fixation of the buoy to the mooring cable was increased by one meter, and the stabilizing moment increased.
- The materials used in the upper part of the buoy were changed from aluminium to carbon composite., reducing the super-structure weight.

A.5 Mooring line from initial deployment

The mooring line used in the initial deployment was left on site, with buoyancy attached. It is reported that divers inspected the mooring line monthly. On the second deployment, however, the mooring line had disappeared.

A.6 Second installation

The modified version of the buoy was deployed on site with all its instrumentation the 16 of May, 2002.

A.7 Loss of the Buoy

May 16 2002: Buoy deployment

The deployment procedure was the same than for the first deployment, except for the following items:

- The main Kevlar cable was short by 40 meters.
- The missing length was replaced by chains. The corresponding weight is estimated to be about 550 kg.
- When leaving the site, the buoy was floating at its nominal floatation line.

May 20-21-22 : Inspection by ship

The buoy was somewhat pushed down (about 1 meter). This was interpreted as being due to the lack of buoyancy of the system (because of the 500 to 600 kg of chains). Part of the deepening was also interpreted as being due to the current (bad weather on the 22 of May, with a wind of 25 knots).

May 27, 2002 : Helicopter survey

The ARGOS beacon stopped its emission of data on the 24 of May. A helicopter survey was carried out the morning of the 27 of May. The buoy was located. All systems were working nominally. The buoy was now pushed down by about 4 meters (the buoy cap was alternatively below and above water (wind speed 25 knots, waves about 2 meters).

May 29, 2002 : Inspection by ship

The buoy was located, floating at the same level as 2 days before.

June 3, 2002 : Helicopter survey

The buoy was again located, floating at the same position and with the same deepening.

June 11, 2002 : Attempt to install additional buoyancy

The buoy could not be located in spite of a 3-hours survey on the site (visual survey + sounder), and was deemed to have sunk.

June 13-14-15 2002 : Attempt to recover the buoy.

Several hours of sonar search failed to locate the buoy. The acoustic releases were triggered, and the bottom part floated to a depth of about 200 meters, with the complete system floating upside down. The acoustic releases and associated floatation devices were secured by dragnet and by ringing around the position. The Kevlar line broke during recovery, and the buoy was lost.

Appendix B RIFLEX PROGRAM DESCRIPTION

B.1 General

RIFLEX is a tailor-made computer program system for static and dynamic analysis of flexible riser systems and other slender marine structures developed by MARINTEK in co-operation with NTNU, the Norwegian University of Technology and Science.

Important properties of slender marine structures are:

- Small bending stiffness
- Large deflections
- Large upper end motion excitation
- Nonlinear cross section properties
- Complex cross section structure
- Normally, a simple system geometry

User friendliness is achieved by taking advantage of the simple system geometry that allows for very simple input/output specifications and automatic mesh generation. Special input/output specifications are available for standard riser systems such as the Free Hanging, Steep Wave, Lazy Wave, Steep S and Lazy S configurations. Several alternatives are available for static and dynamic analyses from very simple methods that are useful in the early stages of design, to advanced 3-D analyses of systems with arbitrary topology.

The main features of the RIFLEX computer program are given by:

- Flexible modelling of simple as well as complex riser systems.
- Nonlinear cross section properties.
- Seafloor friction.
- Material hysteresis models.
- The effective tension concept is applied to account for loading due to internal and external hydrostatic pressure.
- Both beam and bar elements are available for riser modelling.
- The finite element formulation allows for unlimited translations and rotations in 3-D space.
- Nonlinear and linear time domain dynamic analysis.
- Nonlinear static analyses utilising catenary start configurations for simple configurations.
- Eigenvalue analysis to determine natural frequencies.
- Simple analysis options for parametric studies as well as advanced analyses for design verification are available.
- System loading may comprise regular or irregular waves, vessel motions and arbitrary current profiles.
- Simultaneous excitation from several support vessels.
- Hydrodynamic loading is described by the generalised Morison equation including the relative pipe/water particle velocity.

- Special analysis options are available, such as slug flow, release/rupture, restart, transient dynamic loads.
- Identification of contact problems between flexible risers and other subsea installations.
- Optionally, a generalised loading sequence can be used in the static finite element analysis. Useful for "troublesome" systems.
- Hydrodynamic load model for partly submerged, floating elements.
- Modified wave kinematics to account for platform diffraction effects.

RIFLEX has been used to analyse a variety of flexible riser systems. In addition, related slender body systems have been analysed:

- Tensioned steel risers.
- Static and dynamic analysis of anchor lines, including clump weights and buoyancy modules.
- ROV umbilical configurations.
- Fish cage systems, including floating, flexible pontoons.
- Deepwater power cable installations.
- Offshore loading systems.

The RIFLEX program system comprises six separate programs each having their specified task. The programs communicate through a file system.

INPMOD - input module
STAMOD - static analysis
DYNMOD - dynamic time domain analysis
FREMOD - frequency domain analysis
OUTMOD - extract results
PLOMOD - graphic result presentation

INPMOD, STAMOD, DYNMOD, FREMOD and OUTMOD are batch-oriented programs while PLOMOD is interactive.

B.2 Riser System Modelling

A 'top-down' modelling approach is used:
- Specify topology and boundary conditions.
- Specify line composition.
- Specify cross-section properties and discrete components.

The topology specification is available at two levels:
- 'Standard systems' which incorporates the topology and boundary conditions of some of the simplest and most standard riser systems, such as Steep Wave, Lazy Wave, etc.
- 'Arbitrary system' for which the user has to specify topology, boundary conditions and also a stress free condition.

The seafloor contact may be modelled either as one attachment point, or as a tangent plane specification with vertical bilinear springs and horizontal bilinear springs and friction forces in the axial and the lateral directions.

Connectors are used for modelling of hinges and swivels. Boundary conditions for 3 rotational degrees of freedom can be specified as free or fixed in a local coordinate system with coordinate axes defined from the neighbouring elements.

Lines are composed of one or more segments. Each segment is a uniform piece of line. Concentrated forces, such as clump weights and buoys, may be attached at segment intersections. Connectors may also be introduced at segment intersections.

Cross section properties are specified in terms of area, mass and stiffness. Rotation symmetric as well as bi-symmetric cross sections are available. Due to the very complex cross sections in flexible pipes, a global cross-sectional stiffness model is applied in RIFLEX. This means that cross section properties such as axial, bending and torsional stiffness must be specified as input. Furthermore, structural response is always computed as global deformations and stress resultants (axial force, moments). Hence, local strains and stresses in different cross section layers and materials are not considered. Nonlinear cross section behaviour is modelled by introducing nonlinear relations between global deformation parameters and stress resultants, i.e. axial force versus axial elongation, bending moment versus curvature and torsional moment versus twist angle. Cross-sections with bending stiffness will be modelled with 12 DOF beam elements. If zero bending stiffness is specified, a 6 DOF bar element will be used for modelling of the cross section.

Hydrodynamic loading is modelled by means of drag- and inertia force coefficients in longitudinal and transverse directions. Both quadratic and linear drag terms can be included.

B.3 Environment and Excitation ModellingWaves can be modelled in various ways:

- Model spectra (Pierson-Moscowitz, JONSWAP, etc.) and numerically defined spectra.
- Unidirectional and short-crested sea.
- Wind sea and swell.
- Regular waves, Airy waves and Stoke's 5th order waves.

Current is modelled by a current profile with specified current velocity and direction at a set of water levels. A dynamic current variation may be specified.

Forced motions at vessel attachment points are modelled either by specifying vessel motion transfer functions or by specifying motion amplitudes and phase angles directly. Simultaneous excitation from several support vessels can be included in the dynamic analysis. Low frequency motion can be superimposed to the 1st order vessel motions.

B.4 Analysis Options

STAMOD - Static analysis. Depending on system complexity, one may use catenary analysis, finite element analysis, or a combination, using the catenary analysis result as start point for the FEM analysis.

A special parametric variation option is also available for efficient investigation of the static system behaviour by variation of vessel position, current velocities and external forces.

Some of the static analysis results are given directly as print, but most of the results are stored on file for presentation by the output module OUTMOD.

DYNMOD - Dynamic analysis comprises eigenvalue analysis and time domain simulation of dynamic responses.

The eigenvalue analysis calculates mode shapes and natural frequencies for the riser system.

The time domain analysis calculates dynamic motions and forces due to support vessel motions, waves, and current. A wide range of modelling- and analysis options is available:

- Regular or irregular excitation
- Different wave loading models: Airy waves (regular and irregular),Stoke's wave (regular), loads to still water level or to actual water level (regular waves)
- System stiffness, mass and damping matrices updated during the analysis (“nonlinear”) or kept constant during the analysis (linearised analysis)
- Slug flow in gas risers
- Disconnect or rupture simulation
- Restart with change of time steps, damping etc.
- Transient dynamic loads

The nonlinear dynamic analysis is based on an incremental equilibrium formulation which allows for including nonlinear effects due to geometric stiffness, hydrodynamic loading, nonlinear material properties, slug-flow and seafloor interaction. In the linearised dynamic analyses the system matrices (stiffness, mass and damping), are linearised at the static equilibrium position. The nonlinear external load described by the generalised Morison equation is, however, included.

The results from the dynamic analysis are stored on files for subsequent postprocessing by the analysis module OUTMOD.

FREMOD – frequency domain analysis comprises long-term frequency domain analysis of the seastates in described by a scatter diagram. Separate frequency domain analyses with stochastic linearisation may be performed for each seastate or for user-defined blocks of seastees.

The FREMOD results may be used to estimate long-term fatigue damage. Alternatively, frequency domain analyses bay be used to identify seastates with large contributions to the long-term extreme response for subsequent nonlinear time domain simulations.

B.5 Result Post-processing and Output

A special post-processing module OUTMOD is used to select data from the stored results and to prepare statistics, response spectra etc. The output is presented as printed tables or as plots. The user controls the type, form and amount of generated output through the input file. In addition, the user controls the amount of data stored for subsequent post-processing by specifying storage frequency and elements for which results are stored. The following output is available:

- Static system information.
- Static coordinates.
- Final static forces.
- Parameter variation, coordinates and forces.
- Irregular excitation information: Fourier components, wave elevation, vessel motion time series.
- Dynamic snapshot plots of riser motion, wave- and vessel contour.
- Time series of displacements and forces, including distributions and spectral analysis (irregular excitation).
- Envelope curves of motion and forces (regular analysis) or standard deviations (irregular analysis).
- Derived responses, such as element angles, curvature, support forces.
- Initial axial forces and coordinates from the static catenary analysis.
- Line interference (clearance) analysis.
- Fatigue damage calculation using user-specified SN-curves following a time or frequency domain analysis.

A self-contained, interactive plotting module, PLOMOD, is used for presentation of graphs prepared by OUTMOD. The standard graphical system GPGS is used, and drivers for the most commonly used graphics devices are available.

Animation is available in PLOMOD to show system behaviour in terms of riser motions, waves and vessel motions.

For special purposes, the output files can be accessed by other statistics programs, e.g. STARTIMES.

Key results from static and dynamic analysis may also be stored for plotting by the RIFLEX for Windows or MatrixPLot on Windows NT/95.

B.6 Validation

Validation of RIFLEX has been carried out by comparison to analytical solutions, general purpose finite element programs, model tests and full scale measurements.

The main references to the validation studies are:

1. Comparison to analytical solutions:

   SINTEF (1995c), Sødahl (1991)

2. Comparison to other computer programs:

   SINTEF (1995c), Engseth et al. (1988)
   Kodaissi et al (1990), Larsen (1991)

3. Comparison to model tests and full scale measurements:

   Otteren and Hanson (1990), Cook and Fylling (1990),
   Bech and Skallerud (1992), Sødahl et al (1992),
   Fylling et al (1992), Kaasen and Nordsve (1993).

A large number of verification studies were carried out during the development of the RIFLEX program system. A summary of the most important test cases are presented in the RIFLEX test manual (SINTEF 1995c) In addition, RIFLEX has been extensively used for several years by the members of the RIFLEX User Group for design and analysis of actual riser systems. Experiences gained by the User Group have provided most valuable information for validation and development of the RIFLEX program system.

B.7 References

1. Bech, A. and Skallerud, B., (1992):
"Structural Damping in Flexible Pipes: Comparisons Between Dynamic Tests and Numerical Simulations", 2nd International Offshore and Polar Engineering Conference, San Francisco, 1992.

2. Bech, A., Skallerud, B. and Sødahl, N., (1992):
"Structural Damping in Design Analysis of Flexible Risers", Marinflex 92, London, November 1992.

3. Cook, H. and Fylling, I.J., (1990):
"Flexible Riser Behaviour and Modelling", EUROMS '90, European Offshore Mechanics Symposium, Trondheim, Aug. 1990.

4. Engseth, A., Bech, A. and Larsen, C., (1988):
"Efficient Method for Analysis of Flexible Risers". BOSS '88, Behaviour of Offshore Structures, Trondheim, 1988.
* Description of methods, comparison of results with other programs.

5. Fylling, I.J., (1988):
"Design Methods for Deep Water Anchor Systems", Stationkeeping of Platforms and Ships, the Norwegian Society to Chartered Engineers, Fagernes, Nov. 88.
* Anchor line dynamics. Comparison of alternative analysis methods.

6. Fylling, I.J., Sødahl, N. and Bech, A., (1988):
"On the Effects of Slug Flow on the Dynamic Response of Flexible Risers". 4th International Conference on Floating Production Systems, IBC Technical Services, London, Dec. 1988.
* Parameter study of slug force effects on submerged flexible risers by means of RIFLEX.

7. Fylling, I.J. and Bech, A., (1991):
"Effects of Internal Friction and Torque Stiffness on the Global Behaviour of Flexible Risers and Umbilicals". OMAE, Stavanger, 1991.

8. Fylling, I.J., Stansberg, C.T. and Mo, K., (1992):
"Extreme motions and anchor line loads in turret mooring systems". Boss '92, Behaviour of offshore structures, London, July 1992.
* Validation of anchor line dynamics by comparison to model tests.

9. Hanson, T.D., Otteren, A. and Sødahl, N., (1994):
"Response calculation using an enhanced model for structural damping in flexible risers compared with full scale measurements." Proceedings of the international conference on hydroelasticity in Marine Technology, Trondheim.

10. Kaasen, K.E. and Nordsve, N.T., (1993):
"Comparison between measured and simulated dynamic responses of a power cable." OTC, Houston, 1993.

11. Kenison, R.C. and Farrand, A.J., (1989):
"An Assessment of Flexible Riser Behaviour". OMAE '89, 8th International Conf. on Offshore Mechanics and Arctic Engineering, Haag, the Netherlands.

12. Kodaissi, E., Le Marchand, E. and Narzul, O., (1990):
"State of the Art on Dynamics Programs for Flexible Riser Systems". OMAE '90, Offshore Mechanics and Arctic Engineering Conference, Houston, USA.

13. Larsen, C.M., (1991):
"Flexible Riser Analysis - Comparison of Results from Computer Programs". Eng. Structures, 1991.

14. Larsen, C.M., Leira, B.J., Olufsen, A.N. and Sødahl, N., (1992):
"Design Methods for Flexible Risers", BOSS '92, Behaviour of Offshore Structures, London, July 1992.

15. Leira, B.J. and Olufsen, A.N., (1992):
"Application of Frequency Domain Procedures for Flexible Riser Analysis", 2nd International Offshore and Polar Engineering Conference, San Francisco, 1992.

16. Leira, B.J., Olufsen, A.N. and Guoyang, J., (1992):
"Reliability Analysis of Flexible Riser Systems", 2nd International Offshore and Polar Engineering Conference, San Francisco, 1992.

17. Lie, H., Sortland, B. and Lian, W., (1989):
"Design of ROV Umbilical Configurations to Improve ROV Operability". OMAE '89, 8th International Conference on Offshore Mechanics and Arctic Engineering, Haag, the Netherlands.
* Static and dynamic analysis of ROV umbilicals to optimize configurations in order to reduce wave- and current loads on ROVs.

18. Lie, H. and Sødahl, N., (1993):
"Simplified dynamic model for estimation of extreme anchorline tension." Offshore Australia 1993, Melbourne. (To be presented.)

19. Ormberg, H., (1991):
"Non-Linear Response Analysis of Floating Fish Farm Systems." Dr.ing. Thesis, Div. of marine Structures, The Norwegian Institute of Technology, Trondheim, 1991.

20. Otteren, A. and Hanson, T.D., (1990):
"Full Scale Measurement of Curvature and Motions on a Flexible Riser and Comparison with Computer Simulations", OMAE '90, Offshore Mechanics and Arctic Engineering Conference, Houston, 1990.
* Measurements and analysis of the PETROJARL riser on the Oseberg Field.

21. Passano, E., (1994):
"Efficient Analysis of Nonlinear Slender Marine Structures", Dr.ing. Thesis, Dept. of Marine Structures, The Norwegian Institute of Technology (NTH), Trondheim, 1994.

22. Sandvik, P.C., (1994):
"Undervanns kranoperasjoner på ekstremt store dyp", Offshore marine operasjoner, NIF, Oslo 1994 (in Norwegian).

23. SINTEF 1995(a):
"RIFLEX - Flexible Riser System Analysis Program, Theory Manual". MARINTEK and SINTEF, Division of Structural Engineering, Trondheim, Norway.

24. SINTEF 1995(b):
"RIFLEX - Flexible Riser System Analysis Program, User Manual".
MARINTEK and SINTEF, Division of Structural Engineering, Trondheim, Norway, 1987.

25. SINTEF 1995(c):
"RIFLEX - Flexible Riser System Analysis Program, Test
Manual": MARINTEK and SINTEF, Division of Structural Engineering,Trondheim, Norway, 1987.

26. Sødahl, N. and Larsen, C.M., (1989):
"Design Procedure for Bending Stiffeners in Flexible Riser Systems". PRADS '89, Practical Design of Ships and Mobile Units, Varna, Bulgaria, Oct. 1989.

27. Sødahl, N., (1991):
"Methods for Design and Analysis of Flexible Riser Systems". Dr.ing. Thesis, Div. of Marine Structures, the Norwegian Institute of Technology (NTH), Trondheim, 1991.

28. Sødahl, N. and Larsen, C.M., (1992):
"Methods for Prediction of Extreme Responses of Flexible Risers.", 2nd International Offshore and Polar Engineering Conference, San Francisco, 1992.

29. Sødahl, N., Hanson, T.D., Otteren, A. and Fylling, I.J., (1992):
"Influence from Nonelastic Material Modelling in Computer Simulation of Flexible Risers Verified by Full Scale Measurements." Offshore Technology Conference, Houston, 1992.

30. Sødahl, N. and Fylling, I.J., (1992):
"The Riflex Flexible Riser Analysis Program", Marintek Review, No. 1, 1992.

31. Leira, B.J. and Mathisen, J., (1995):
"Reliability-based Safety Factors for Flexible Risers", Proc. OMAE'95, Copenhagen.

32. Karunakaran, D., Olufsen, A., Nordsve, N.T. and Leira, B.J., (1995):
"Flexible Risers Configuration for a FPSO in Deep Waters", Proc. OMAE'95, Copenhagen.

33. Hanson, T.D. and Nilsen, A.U., (1995):
"Probabilistic Design of a 15" Flexible Riser", Proc. OMAE'95, Copenhagen.

Appendix C GLOBAL CALCULATION MODEL

The present numerical model is made with the purpose to model the buoy and the mooring system with high enough accuracy to capture the overall global behaviour of the system when it is exposed to environmental loading, and to calculate the eigen frequencies of the rigid buoy modes. This requires that buoyancy; inertia and stiffness properties are correctly modelled, while the local structural details are of less concern. Added mass and drag coefficients that corresponds to the real structure must however be applied.

The anchor line used consisted of 6 different segments of various lengths and properties. The bottom segments was a chain section, the kevlar rope covering the bulk part of the total length followed this segment, and on the upper end four different chain segments lay between the kevlar and the buoy. In the numerical model, 5 segments are used in the finite element model of the mooring line. A 2m long chain segment is put into segment 3. Bending- and torsional stiffness in the mooring line is negligible. Table C.1 below gives the main properties of the mooring lines as modelled. The segments are numbered from bottom to top so that segment 2 is the kevlar rope. Note that the given lengths are unstretched lengths.

The weights of the acoustic releases and the other elements of the coupling system are included as distributed weights for the bottom end chain section. The chains at the top end were modelled as three segments, where the weight of shackles is included as distributed weights on the middle segments (Segment 4).

Table C.1 Numerical FE-model of mooring line.

Designation	Unit	Segment 1	Segment 2	Segment 3	Segment 4	Segment 5
Length	m	35	2311.2	24	12	25
Axial stiffness, EA	kN	3.0E+05	4040.0	3.0E+05	3.0E+05	3.0E+05
Unit weight, dry	kN/m	9.75E-02	1.43E-03	5.59E-02	0.221	5.59E-02
Unit weight,subm.	kN/m	8.27E-02	7.68E-05	4.86E-02	0.193	4.86E-02
Diameter	m	1.60E-02	1.31E-02	1.60E-02	3.2E-02	1.60E-02
Added mass coeff.	-	2.0	1.0	2.0	2.0	2.0
Drag coeff.	-	2.0	1.2	2.4	2.4	2.4
No. of elements	-	5	30	4	2	4

The buoy comprises three beam element segments: the lower aluminium truss beam, the upper aluminium truss beam and the antenna (structure made of carbon fiber). For the buoy bending- and torsional stiffness is important. The weight of each segment is distributed evenly out along each segment and the cross-section properties at the middle of each segment are used for the entire segment. It is reported that the total weight of instrumentation and equipment on the buoy amounted to 250kg. In the BSMEM report, Genimar lists instrumentation and equipment of total

200kg with their corresponding vertical position. These are treated separately (see below), while the additional 50kg are evenly distributed along the carbon structure.

Table C.2 gives the main properties of the buoy as modelled. The segments are numbered from bottom to top so that segment 3 is the carbon structure.

Table C.2 Numerical FE-model of mooring line.

Designation	Unit	Segment 1	Segment 2	Segment 3
Length	m	1.8	9.0	13.0
Axial stiffness,EA	kN	4.17E+05	4.17E+05	4.61E+05
Bending stiffness, EI	kNm^2	1.26E+05	1.38E+05	2.88E+04
Torsional stiffness, GI	kN/m	1.00E+05	1.00E+05	1.00E+05
Unit weight, dry	kN/m	0.406	0.406	9.43E-02
Unit weight,subm.	kN/m	9.02E-02	9.02E-02	-8.29E-03
Diameter	m	0.10	0.10	0.057
Radius of gyration	m	0.55	0.575	0.25
Added mass coeff.	-	4.0	4.0	4.0
Drag coeff.	-	4.8	4.8	4.8
No. of elements	-	3	10	10

The diameters listed above are only used for computation of added mass and drag force. They are therefore set to be the diameter of one of the four corner pipes, while the added mass and drag coefficients are set to be four times the value for a single pipe. This way the computed added mass and drag force should represent to true values in a satisfactory manner. The torsional stiffness is not known and is therefore set to a large value. Torsion is not an important response in the current design.

The sphere is modelled as a body that is connected to a selected node. Here it is placed at the intersection between segment 1 and 2. A mass, a volume and added mass and drag coefficients describe the body. The mass of the sphere is 136kg and its volume is $3.05m^3$. Added mass of a sphere in an unbounded fluid is equal to half of the mass of the displaced fluid. The sphere is located sufficiently far from the free surface for this to be valid, and the hydrodynamic mass is thus 1563kg in the translatory degrees of freedom (surge, sway and heave). The added mass is also utilized when computing the wave excitation force on the buoy.

Since the heave motion has its natural period in a region of high wave energy, the heave damping is crucial for the heave response. The major damping contribution comes from drag on the sphere. For a sphere in a constant current the drag coefficient is approximately 0.5 and this value is used in the calculation of the buoy exposed to constant current. In oscillatory flow however the drag coefficient is strongly dependent on the Keulegan-Carpenter number (KC-number). For the present case the KC number is small which yields a large drag coefficient. In simulations presented in this work, C_D=5 is used for the sphere. Sensitivity of the results to chice of C_D have

been studied by numerical decay tests. The results are not particularly sensitive to C_D and the analyses should provide results in the right order of magnitude.

The instrumentation and equipment listed in BSMEM report by Genimar are also treated as one body of 200kg. This is located at a vertical position so that the body gives an equivalent inertia moment as the sum of the different parts. A buoyancy tank was added at the junction between the aluminium- and carbon structure. This is modeled as a vertical nodal force of 1000N.

Appendix D RESULTS FROM HYDRODYNAMIC ANALYSES

Results from simulation of the buoy for the original buoy design in irregular sea. In Case 4 the distance between fairlead and center of buoy is increased by 1 metre (modified design).

Case 1: Original buoy design, sea state no.1 : H_S = 1.5m, T_Z=7.0s.
Case 2: Original buoy design, sea state no.2 : H_S = 3.5m, T_Z=9.0s.
Case 3: Original buoy design, sea state no.3 : H_S = 6.0m, T_Z=10.0s.
Case 4: Changed buoy design, sea state no.2 : H_S = 3.5m, T_Z=9.0s.

Table D.1 Motion response of buoy

	Mean	St.dev.	Skewness	Kurtosis	Min.(3hrs)	Max.(3hrs)
Case 1						
Surge (m)	0.477	0.836	-0.094	2.846	-2.832	3.179
Heave (m)	0.000	0.523	-0.035	2.809	-1.923	1.958
Pitch (deg)	0.186	1.855	0.093	2.634	-4.510	5.948
Case 2						
Surge (m)	0.700	1.366	0.053	3.089	-4.577	6.481
Heave (m)	0.000	0.998	-0.011	2.963	-4.219	3.533
Pitch (deg)	0.770	2.390	0.263	3.011	-6.254	11.33
Case 3						
Surge (m)	3.916	2.306	-0.140	3.038	-4.694	11.61
Heave (m)	0.00	1.589	-0.011	3.058	-6.784	6.150
Pitch (deg)	2.063	3.593	0.599	3.730	-7.657	18.39
Case 4						
Surge (m)	1.678	1.383	0.079	3.069	-3.438	7.536
Heave (m)	0.000	0.992	-0.019	2.975	-4.232	3.529
Pitch (deg)	0.504	1.722	0.220	2.777	-4.612	8.522

Table D.5 Tension in top end and in bottom end of kevlar rope.

	Mean	St.dev.	Skewness	Kurtosis	Min.(3hrs)	Max.(3hrs)
Case 1						
Ten. top (kN)	22.64	0.755	-0.015	2.782	19.93	25.57
Ten. bot. (kN)	22.47	0.891	-0.022	2.816	19.19	25.87
Case 2						
Ten. top (kN)	22.65	1.412	0.012	2.896	16.96	27.55
Ten. bot. (kN)	22.48	1.705	0.003	2.973	15.28	28.57
Case 3						
Ten. top (kN)	22.66	2.222	0.020	2.982	13.52	31.12
Ten. bot. (kN)	22.49	2.714	0.004	3.064	10.97	33.12
Case 4						
Ten. top (kN)	22.73	1.508	-0.003	2.904	16.56	27.98
Ten. bot. (kN)	22.56	1.813	-0.003	2.984	14.84	29.08

Table D.6 Shear force (kN) in the different cross-section of buoy.

	Mean	St.dev.	Skewness	Kurtosis	Min.(3hrs)	Max.(3hrs)
Case 1						
Position 1	0.015	0.161	0.105	2.745	-0.550	0.615
Position 2	0.014	0.145	0.092	2.737	-0.487	0.552
Position 3	0.012	0.148	0.017	2.465	-0.463	0.500
Case 2						
Position 1	0.054	0.233	0.043	2.717	-0.702	1.039
Position 2	0.052	0.213	-0.024	2.694	-0.656	0.925
Position 3	0.049	0.215	-0.056	2.523	-0.633	0.728
Case 3						
Position 1	0.135	0.309	0.021	2.782	-0.899	1.295
Position 2	0.130	0.282	-0.073	2.780	-0.847	1.136
Position 3	0.130	0.290	-0.028	2.725	-0.855	1.167
Case 4						
Position 1	0.051	0.395	0.018	2.624	-1.308	1.613
Position 2	0.049	0.376	- 0.011	2.607	-1.262	1.511
Position 3	0.023	0.170	0.011	2.708	-0.513	0.734

Table D.7 Bending moment (kNm) in the different cross-section of buoy.

	Mean	St.dev.	Skewness	Kurtosis	Min.(3hrs)	Max.(3hrs)
Case 1						
Position 1	-0.163	1.781	-0.041	2.536	-6.198	5.683
Position 2	-0.149	1.694	-0.040	2.536	-5.969	5.356
Position 3	-0.057	0.777	-0.189	2.767	-3.441	2.306
Case 2						
Position 1	-0.681	2.755	-0.015	2.673	-10.41	8.18
Position 2	-0.633	2.607	-0.041	2.702	-10.13	7.71
Position 3	-0.282	1.229	-0.571	3.840	-7.48	3.07
Case 3						
Position 1	-1.814	3.879	-0.120	2.943	-16.26	11.10
Position 2	-1.693	3.683	-0.177	3.024	-16.02	10.34
Position 3	-0.801	1.930	-1.167	5.911	-13.41	4.20
Case 4						
Position 1	-0.620	3.565	0.009	2.515	-12.40	11.41
Position 2	-0.579	3.301	-0.015	2.524	-11.73	10.40
Position 3	-0.274	1.395	-0.779	4.300	-8.444	3.079

Position 1 = Middle of aluminium sphere
Position 2 = Intersection between tubes and sphere
Position 3 = Transition between aluminium structure and carbon fibre

Appendix E DETAILED CALCULATION MODEL

The stress in the sphere shell is found for different load cases. The coordinate system in which the results are given, is shown in Figure 27c. The FE-model is fixed along the edges of the sphere shell. The lower end of the tube in the detailed FE-model is located at the joint between the different members in the tubular structure. Two different sets of boundary conditions are applied to this end (see Figure 27d and e). For BC1, the tube end is free. Hence, any load applied to the tube is carried only by the sphere shell. This boundary condition is used to represent the behaviour of the structure when heave motion is dominating (buoyancy forces applied to the sphere is balanced by inertia forces in the tubular structure). When the motion of the structure is pitching, the forces on the tubular structure induced large deflections of the members relative to each other. In this case, BC2 for which the joint prevent displacements of the end of the tube is most representative.

The upper end of the tube is subjected to axial load as shown in Figure 28. The axial stress is found at the two sides of the plate representing the inside and the outside of the sphere. The largest stress is found at the lower edge of the intersection between the sphere and the cylinder.

The fatigue capacity of the connection is given by the SN-curve,

$$N = N_{ref} \times \left(\frac{s_{ref}}{s} \right)^m$$

where s is the stress range, N is the predicted number of cycles to failure, m is the inverse slope of the SN-curve. With m equal to 3.2 and fatigue class 18 for the detail in question, the fatigue life is $N_{ref} = 2 \cdot 10^6$ cycles for a stress range equal to $s_{ref} = 18$ MPa.

When the buoy is subjected to variable amplitude loading, the stress maxima in a short term sea state are Rayleigh distributed. An equivalent stress range is then found as

$$s_{\text{eq}} = \Gamma\left(1 + \frac{m}{2}\right)^{1/3} 2\sqrt{2}\sigma_s .$$

The mean zero-crossing period is taken as 7 s (seastate 1). The maximum allowed standard deviation for different life times is shown in Table 2.

Appendix F RESULT PLOTS FROM SIMULATION OF SEASTATE 1: H_S=1.5M, T_Z= 7.0S

Appendix G RESULT PLOTS FROM SIMULATION OF SEASTATE 2: H_S=3.5M, T_Z= 9.0S

Appendix H RESULT PLOTS FROM SIMULATION OF SEASTATE 3: H_S=6.0M, T_Z= 10.0S

Appendix I RESULT PLOTS FROM SIMULATION OF CASE 4 (MODIFIED DESIGN UNDER SEASTATE 2): H_S=6.0M, T_Z= 10.0S